공학석사 학위논문

Design of a greenhouse energy model including energy exchange of internal plants and its application for energy loads estimation

작물 에너지교환을 고려한 온실 에너지모델 설계 및 에너지부하 산정

2017 년 2 월

서울대학교 대학원

생태조경 · 지역시스템공학부 지역시스템공학전공

이 승 노

Design of a greenhouse energy model including energy exchange of internal plants and its application for energy loads estimation

작물 에너지교환을 고려한 온실 에너지모델 설계 및 에너지부하 산정

지도교수 이 인 복

이 논문을 공학석사 학위논문으로 제출함
2017 년 2 월

서울대학교 대학원
생태조경 · 지역시스템공학부 지역시스템공학전공
이 승 노

이승노의 공학석사 학위논문을 인준함
2017 년 2 월

위 원 장 _____(인)

부위원장 _____(인)

위 원 _____(인)

Abstract

The greenhouse cultivation in South Korea has increased dramatically in the past few decades and most of the greenhouses use fossil fuel as an energy source. As interest in new energy sources that can replace fossil fuel has increased globally in recent years, the greenhouse industry in South Korea has also attempted to utilize renewable energy for heating and cooling systems. Moreover, it is important to analyze energy use in greenhouses by crops species and growing stage to determine how the new energy source will be utilized. However, greenhouse energy loads have been calculated by assuming that the crops are not in cultivation or without considering the characteristics of each crop using prior research, in spite of that a large portion of radiation which penetrates the cladding use for crop transpiration. As energy exchange by crops take a large part in greenhouse energy balance, there should be a quite difference in energy loads whether the energy exchange by crops is considered.

In this thesis, the dynamic energy exchange model of greenhouse was designed to calculate greenhouse energy loads hourly for the essential prerequisite to apply new energy source in the greenhouse. Literature reviews were conducted for a calculation method to build energy consumption, an energy balance equation to simulate the greenhouse environment, and a model for energy exchange by crop. These were used as methodology for the model design. As a result, a dynamic analysis method was used to design the greenhouse energy model and the empirical equation by Stanghellini (1987) was used to realize the energy exchange between crops and ambient air in the greenhouse.

The target was an eight-span plastic-covered greenhouse, which applied thermal effluent from a nearby thermal power plant on a trial basis as a heat source of the heat pump. Field experiments were conducted to collect the greenhouse structural characteristics, working schedule of the heating, ventilating and air conditioning (HVAC) system, and crops characteristics for the design and validation

of the dynamic energy exchange model of greenhouse. The greenhouse energy model was designed by using one of the commercial building energy simulation programs TRNSYS (Transient Systems Simulation Program). The entire greenhouse energy model was designed in three parts: greenhouse structure modeling, crops energy exchange modeling, and thermal effluent – heat pump modeling based on measured data. To realize the energy exchange by crops, the average leaf area index (LAI) of cultivated crops in the greenhouse was measured. Then, the regression equation of the stomatal resistance was derived. The micro-climate data inside and outside the greenhouse, which include solar radiation, and air temperature, were also used to validate the greenhouse energy model. The crop transpiration rate was used to validate the energy exchange model of the crop while the greenhouse internal air temperature was used to validate the entire greenhouse energy model. As a result, the designed crops energy exchange model provides a good estimate of the transpiration rate throughout the experimental period ($R^2 = 0.96$, $d = 0.99$) and the designed dynamic energy exchange model of greenhouse provides a good estimate of the greenhouse internal air temperature ($R^2 = 0.97$, $d = 0.99$).

The validated dynamic energy exchange model of greenhouse was used to calculate the hourly greenhouse energy loads based on 10-years of weather data. The periodic energy loads were calculated by the sum of the hourly data based on the Irwin mango growth period and the maximum energy loads found for each period. The periodic energy loads were used to analyze the energy cost by two energy sources: the kerosene boiler and the thermal effluent – heat pump system. The average energy cost when using the thermal effluent – heat pump system was analyzed to be 68.21% lower than the kerosene boiler. The proper performance of heat pump was calculated according to the design standard which was provided by National Institute of Agricultural Engineering (NIAE) of the Rural Development Administration (RDA) of South Korea. It suggests that the proper performance of heat pump in greenhouse should be 70% of the maximum cooling and heating loads of last five years. The maximum cooling and heating loads of the last five years were

518,703 and 469,872 kJ/hr, respectively, therefore the proper performance of heat pump was calculated as 363,092 kJ/hr in the cooling capacity and 328,910 kJ/hr in the heating capacity. The results were compared with the performance of heat pump installed in the target greenhouse. The rated cooling and heating capacity were designed to exceed about 28.7% and 20.8% of the proper performance, respectively, due to the different method used to calculate the greenhouse energy loads. The effect of crop energy exchange to energy loads was analyzed by comparing the energy loads dependent on the existence of crops. The annual and maximum cooling loads were increased on average by 23.23% and 14.25%, respectively, and the heating loads were decreased on average by 11.02% and 7.56%, respectively, when assuming the crops are not in cultivation. Therefore, the energy exchange between crops and ambient air in the greenhouse should be considered when calculate the energy loads of greenhouse.

Keyword: building energy simulation (BES), energy loads, greenhouse, plant energy exchange model, renewable energy

Student Number: 2015-21756

Contents

List of figures

List of tables

1. Introduction

As South Korea has four distinct seasons, it is hard to produce crops by field culture throughout the year. Greenhouses can control the growing environment of crops and produce high quality crops all through the year. Therefore, the greenhouse cultivation in South Korea increased from 23,669 ha in 1990 to 54,168 ha in 2014. To maintain optimum growing environments for the crop, around 30% of greenhouse utilize the cooling and heating systems. Among them, approximately 85% of all greenhouse farmers use fossil fuel as an energy source (Ministry of Agriculture, Food and Rural Affairs, 2015a).

After the Industrial Revolution, the dependence on fossil fuels increased globally due to the use of petroleum, natural gas, and coal in machines. Moreover, the world population has increased around 1.7% per year for the last 50 years (Ortiz-Ospina and Roser, 2016). As energy consumption per capita increased from 1.46 TOE/year in 1981 to 1.78 TOE/year in 2014, energy consumption around the world has also increased from 6,582.9 million TOE/year to 12,928.4 million TOE/year. Along with a dramatic rise in energy consumption, global issues like global warming, climate change, and energy crunch have arisen and with them, brought interest in new energy sources to replace fossil fuels. Therefore, some attempts have been made to utilize water power, wind power, geothermal heat, and others. While the country has gone through rapid development, energy consumption in South Korea has also increased from 122.0 million TOE/year in 1995 to 213.9 TOE/year in 2014. In addition, due to high population density and lack of natural resources, South Korea imports the 95.2% of total energy consumption in the country (Korea Energy Economics Institute, 2016). Thus, the South Korea government established the Energy Act, Energy Use Rationalization Act, Sustainable Development Act, and others to reduce the total energy consumption and improve energy efficiency. In addition, the Ministry of Agriculture, Food and Rural Affairs provides financial aid

to greenhouse farms that use renewable energy to lower the reliance on imported fossil fuels and improve the efficiency of energy usage (Ministry of Agriculture, Food and Rural Affairs, 2015b).

In South Korea, more than 80% of the total energy production is from thermal power generation or nuclear power generation. During energy production, thermal or nuclear power plants waste around 56% of the total energy input by heating up the engine. The power plant mostly uses seawater to cool down the engine and then discharges the heated seawater, known as thermal effluent. As thermal effluent absorbed the waste heat in the power plant, thermal effluent includes massive thermal energy. Thermal and nuclear power plants around the country discharge around 55.2 billion tons of thermal effluent per year. This includes around 388,000 GWh of thermal energy, which can utilize as energy source. The total amount of thermal energy in thermal effluent can easily cover the entire heating energy for greenhouse in South Korea and can reduce the energy cost in greenhouse (Cho et al., 2010). To use thermal energy in the thermal effluent for the greenhouse heating and cooling systems, various equipment like water storage tanks, heat pumps, heat storage tanks, fan coil unit, and more must be considered (Fig. 1). To use energy more efficiently, each component should be properly designed based on the energy loads of greenhouse. As the amount of available thermal energy in thermal effluent is differing according to the time, the energy loads of greenhouse should be estimated considering the time variable such as season or crop growth stage.

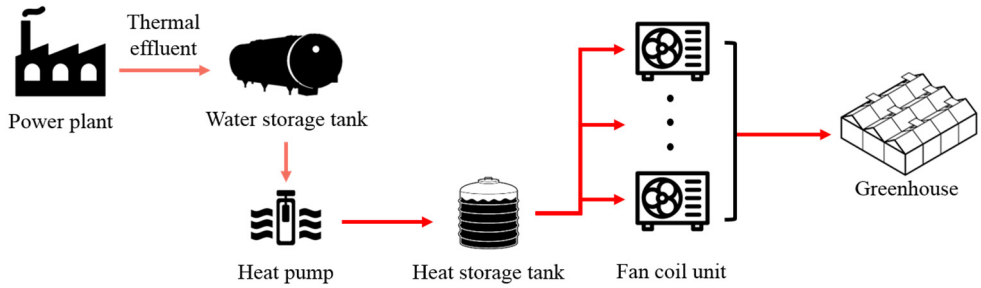

Fig. 1 Outline of thermal effluent utilization in greenhouses

The method of estimating the building energy loads can be divided into a static method and dynamic method according to the time factor. Energy loads are calculated while assuming the indoor and outdoor environmental conditions are in steady-state for a static method. In the case of greenhouses, regardless of type, maximum energy loads can be calculated based on the ambient air temperature and solar radiation in warmest and coldest day. Periodic energy loads can be calculated by the accumulated difference between the optimum growth temperature of cultivation crops and external ambient temperature (Lee et al., 2011; Nam et al., 2015). The static method has a disadvantage in that it does not consider the thermal storage of cladding by solar radiation and internal heat source (Song et al., 2009). This can be a problem particularly in greenhouses as the cladding is much thinner than a general building, so it is much more sensitive to changes in weather conditions. In addition, the energy exchange between crops and soils in the greenhouse and ambient air change drastically over time (Al-Helal and Abdel-Ghany, 2011). Therefore, when calculating energy loads of greenhouses by a static method, there are some differences between the calculated energy loads and actual energy loads. On the other hand, a dynamic method considers the actual energy flow under unsteady state. A dynamic method is the way to calculate energy balance of structure over time based on a numerical analysis. With a dynamic method, energy loads are calculated by simulating the energy exchange considering thermal storage with real

time weather data. The energy balance equation of specific time was analyzed and transmit the amount of energy exchange and thermal storage of each component to next time step. In architecture, a building energy simulation (BES) technique is mostly used as a dynamic method to calculate energy loads due to the high accuracy and capability. Recently, this technique is also used in agriculture to simulate energy exchange in greenhouse dynamically and validate the dynamic energy exchange model of greenhouse (Luo et al., 2005; Sethi, 2009; Candy et al., 2012; Ntinas et al., 2014; Attar et al., 2015). Therefore, it is necessary to use a dynamic method to simulate the energy exchange in greenhouses more precisely by considering the environmental change inside and outside the greenhouse.

In this thesis, a dynamic energy exchange model of multi span plastic covered greenhouse was designed and validated with internal air temperature. A plant energy exchange module was also designed with the micro-climate data of the greenhouse and crop characteristics to simulate the energy exchange between the crops and ambient air. The plant energy exchange module was validated with the measured crop transpiration rate and applied in entire energy model of greenhouse. Based on the validated greenhouse energy exchange model, the maximum and periodic energy loads were calculated by the crop growth stage. Energy loads were calculated for 10 years to analyze the trends according to weather conditions and to derive average energy loads. The hourly energy load data were used to calculate periodic energy loads as well as analyze the energy cost and maximum energy loads to decide the proper scale of a heat pump in the greenhouse. The effect of plant energy exchange in energy loads of greenhouse was analyzed by comparing the cooling and heating loads depending on the existence of crops. The comparative analysis of energy costs was conducted according to an energy source as an essential prerequisite to utilize thermal energy of thermal effluent.

2. Literature Review

2.1. Calculating method for building energy consumption

The method to calculate building energy loads can be classified by the periodic energy loads and maximum energy loads according to the purpose. The periodic energy loads are calculated to estimate the energy cost for a certain period of time and the maximum energy loads are calculated to suggest a proper scale of heating and cooling devices in extreme weather conditions. The calculating method for building energy consumption can also be classified into a static analysis method and dynamic analysis method according to the consideration of time factor. A static analysis method is used to calculate the energy consumption of a building by assuming that the inside and outside environmental conditions are steady state. A dynamic analysis method calculates the building energy consumption by considering the changing environmental condition by time.

A static analysis method includes a Degree-day method and BIN method. By Degree-day method, energy loads of building are calculated based on the degree-day which is the total number of day when the outside ambient temperature is exceed the internal setting temperature or vice versa. Add to this, a BIN method considers the difference between the outside ambient temperature and internal setting temperature and classify them in several groups which is defined as BIN. To calculate the energy loads by the Degree-day method, the heating degree-day (HDD) and cooling degree-day (CDD) should be integrated. HDD and CDD can be defined relative to the difference between outside ambient temperature and internal setting temperature. When the outside temperature is lower than the internal setting temperature on a particular day, the day is included in HDD while in inverse, the day is included in CDD. By using HDD and CDD, the periodic energy loads are calculated on the assumption that the specific heat loss coefficient of the building cladding and temperature differences between outdoor and indoor are uniform during the analysis

period. In addition, the internal heat generation is also assumed to be no proportion in energy balance based on that it is equal to conduction heat loss through the cladding, therefore, this method is less precise (Hong and Cho, 2001). Nonetheless, the Degree-day method is often used to calculate energy loads due to the simple calculation process. For example, Mihara (1978) compensated the heating degree-hours by considering the hours of daylight by regional groups in Japan while Moon and Park (1984) arranged heating degree-days of the main cities in South Korea. Woo et al. (1998) modified the empirical equation for degree-hours which is derived from Mihara (1978) to apply in greenhouses in South Korea using the Degree-day method. Cho et al. (2010) considered the change of internal setting temperature and rearranged the degree-days of the main city in South Korea by analyzing 30-year weather data. Durmayaz et al. (2000) calculated practical energy requirements and fuel consumption of residential building in Istanbul by cooling and heating degree-hours. Similarly, Sarak and Satman (2003) calculated residential heating natural gas consumption in Turkey in terms of degree-days. Christenson et al. (2006) analyzed the impact of a gradually warming climate on the heating and cooling energy demand and degree-days of buildings in Switzerland. Krese et al. (2012) calculated electric energy consumption in building by using the cooling degree-day method and improved the method by considering latent loads.

The BIN method refers to a procedure where the monthly weather data is sorted into discrete groups (bins) of weather conditions, such as ambient dry bulb temperature. The BIN method can consider hourly energy loads, which did not consider in the Degree-day method. As it can be used to calculate the proper scale of the HVAC system using the building energy loads for a specific time period, the BIN method is used to estimate the proper scale of a new HVAC device to evaluate the energy saving technology. Cane (1979) used the modified BIN method to estimate the annual heating energy requirements of residential air source heat pumps to compare with the method recommended by ASHRAE (American Society

of Heating, Refrigerating and Air-Conditioning Engineers). The results are also compared with the experimentally monitored heating energy requirement. The modified BIN method can predict the energy requirement of the building more accurately than the standard ASHRAE method. Kim et al. (1990) developed a software package (KEES; KICT energy estimating system) to calculate the annual energy consumption of the HVAC system in the building based on the BIN method. Thamilseran and Haberi (1994) calculated the energy savings from energy conservation retrofits to HVAC systems based on hourly whole-building electricity, sub-metered motor control center use and thermal energy measurements. Lee and Choi (1997) evaluated the accuracy of the BIN method by comparing with the resistance-capacitance method. Kavanaugh (1998) analyzed the impact of fluid coolers or cooling towers on the GSHP (Ground Source Heat Pump) loop length design, annual ground loop heat buildup, system demand and annual energy use by utilizing the modified BIN method. Parent (2001) developed and validated a simulation model for assessing the feasibility of a GSHP operating tool based on the modified BIN method. Wang et al. (2014) analyzed the energy efficiency retrofit schemes for HVAC systems in office buildings based on the modified bin method.

A dynamic analysis method is the way to analyze real time energy flow of a building based on an energy balance equation by time. This method assumes that the energy exchange by conduction, convection, and radiation affect each other by time. The energy loads are calculated based on the unsteady state, so they can be classified as an analytical method (response factor method, weighing factor method, transfer function method) and numerical method (finite difference method, finite element method, finite volume method) according to the method used to calculate the room temperature change (Hunn, 1996). They can consider variable factors like room thermal capacity, ambient air conditions, solar radiation, internal heat generation, and others. Therefore, by using a dynamic analysis method, the energy flow can be analyzed more precisely by time than a static analysis method. As the

partial differential equation should be solved to calculate building energy consumption by a dynamic analysis method, this method has become common in architecture along with computer technology development. Various energy simulation programs that calculate building energy loads have been developed with the advances in computer technology since the 70's (Hong and Cho, 2001). Commercial dynamic BES programs, such as DOE-2, ESP, TRNSYS, and others have been developed around the world due to the increase of the interest to use energy more efficiently. As various variables should be considered in energy models to use commercial BES programs, specific and accurate pre-processing processes must take precedence. Therefore, research has been conducted to validate the program in different regions and topography (Veken et al., 2004; Karlsson et al., 2007) and different building types (Jensen, 1995; Lomas et al., 1997; Hyun et al., 2002; Reddy et al., 2007).

2.2. Energy balance equation for simulating the greenhouse environment

The greenhouse is a facility that provides a proper environment as ambient temperature, humidity, carbon dioxide concentration, solar radiation, and other factors for plant growing. To control various environmental factors, it is necessary to understand the energy balance in the greenhouse. By this purpose, several researchers analyze the relationship between external weather conditions and internal micro-climates of greenhouse. Whittle and Lawrence (1960) analyzed several factors related to the change of temperature and humidity according to solar radiation. They suggested that the internal air temperature of greenhouse rises in both unventilated and ventilated condition, however, they did not analyze the correlation between increment of air temperature and ventilation rate quantitatively. Walker (1965) developed an analytical procedure to predict the temperatures within both heated and ventilated greenhouses. Cooper (1969a, b) and Papadakis et al. (1989) analyzed the optical properties and thermal radiation at cladding based on the greenhouse energy balance equation. They suggested that the thermal radiation exchange should be considered when greenhouse cladding is consisting of polyethylene cladding unlike with glass cladding. Kimball (1973) developed an energy balance model for various locations in the greenhouse and predict the internal air temperatures and vapor pressures. The model could predict the energy requirements of a greenhouse based on greenhouse properties and external weather conditions. Duncan et al. (1981) developed a greenhouse simulation model that considers solar radiation, conduction heat loss at cladding, ground heat loss, and ventilation heat loss to calculate winter heating requirements and then the data calculated by the conventional degree-day method was compared. Garzoli and Blackwell (1981) calculated the rate of heat loss from a heated single cladding plastic greenhouse. They classified the heat loss of cladding by convection, condensation,

and radiation, and analyzed the various heat transfer processes to estimate the nocturnal heat loss. However, these studies estimated latent and sensible heat from plant and soil by an empirical formula only consisted of a simple factor such as ambient air temperature, transfer coefficient or a rate of total energy flow in the greenhouse, even if such methods were applied in preceding research for specific greenhouse. Seginer and Levav (1971) pointed out that existing steady-state greenhouse energy models have some limitations. The existing energy exchange model for greenhouse consists input data as a primary boundary condition which did not consider the shape and cladding properties of the greenhouse. For instance, in some research, the fixed value of transmittance was used to consist radiation input data, however, it depends on the properties of greenhouse cladding. In addition, Kindelan (1980) indicated that most of the existing models assumed that each element in greenhouse exchange energy with ambient air separately. The thermal storage at each element was also neglected, therefore, the internal air condition of greenhouse immediately changes to the external weather conditions so that steady analysis method was widely used. By this assumption, the response times are not analyzed and can't involve transient processes, which are important in a dynamic energy exchange model. To predict the conditions in a greenhouse by time, a model has to develop with considering the primary environmental conditions and thermal storage of each element (Kindelan, 1980).

The analysis of energy exchange in greenhouse by static method figured out that inaccurate than dynamic method, therefore, many researchers design energy exchange model for greenhouse based on a dynamic energy exchange theory. Ahmadi and Glockner (1982) numerically simulated the thermal performance of plastic-covered greenhouses for winter weather conditions. The greenhouse is modeled by several layers that exchange heat with each other by radiation, convection, and conduction. Bot (1983) developed the greenhouse dynamic energy exchange model to simulate the energy exchange between several elements in

greenhouse such as outside air, cladding, two air layer (air above the screen and below the screen), thermal screen, canopy, and four soil layer. Air exchange by ventilation, radiation, convective heat exchange at cladding, heating pipes, and soil are analyzed based on the physical processes. Moreover, Cooper and Fuller (1983) designed the transient greenhouse energy model by the commercial building energy simulation program. The cover, floor, growing medium, air space, and crop are modeled separately, but interact with each other. Arinze et al. (1984) developed a dynamic analytical thermal model to predict the greenhouse thermal performance. The model predicted the absorbed and transmitted solar energy by greenhouse cladding, inside air, plant canopy, soil and so on. They used this model to evaluate the efficiency of thermal storage system in greenhouse. Singh et al. (2006) developed a computer model to predict the micro-climate of a greenhouse with trickle-irrigated tomato crop. The model consists of a set of algebraic energy exchange equations between cladding, inside air, canopy surface, and bare soil surface. Fitz-Rodriguez et al. (2010) developed a web-based application to simulate a dynamic energy exchange of greenhouses. Even though the model was not fully developed for detail and accuracy, it signified the growing interest in the transient greenhouse energy model analysis. Joudi and Farhan (2015) developed a dynamic model to predict the internal air temperature and soil temperature. They also include heat exchange between soil surface and ambient air in the model to improve the prediction accuracy. However, most researchers assumed that the crops are not in cultivation (Baille et al., 2006; Mesmoudi et al., 2010; Ha et al., 2015; Joudi and Farhan, 2015) or did not consider the crop characteristics and used empirical equation which was derived from preceding research for specific crops (Ahmadi and Glockner, 1982; Bot, 1983; Cooper and Fuller, 1983; Arinze et al., 1984; Singh et al., 2006; Fitz-Rodriguez et al., 2010). The crop energy exchange can be varied depending on species and growing environment. To predict the micro-climate of greenhouses more precisely, various plant characteristics such as LAI, stomatal resistance on leaf surface, growth

period should be considered. In this study, plant characteristics of Irwin mango, which are cultivated in the target greenhouse, are measured and investigated to determine the energy exchange by plants.

2.3. Modeling for energy exchange by crop

A large portion of solar radiation in greenhouses is used for energy exchanges between crops and ambient air. As it can differ by species and plant density, the proportion of energy used for plant energy exchange is in the range of 20 to 75% (Garzoli and Blackwell, 1973; Boulard and Baille, 1987; Kittas et al., 2003, 2005). Al-Helal and Abdel-Ghany (2011) simulated energy flow in the greenhouses and analyzed that around 40% of the external solar and thermal radiation converted to the latent and sensible heat of plants in greenhouse. The energy exchange by solar and thermal radiation above the plants is consists of sensible heat, latent heat, photosynthesis, and thermal storage (Eq. 1).

$$R_n = H + LE + M + J \qquad \text{Eq. 1}$$

Where, R_n is a net flux of radiation above plants (W/m^2), H is a flux of sensible heat between plants and surrounding air (W/m^2), LE is a flux of latent heat due to water evaporation at plant surface (W/m^2), M is a photosynthesis rate stored in the plants (W/m^2), and J is a thermal energy rate stored in the plants (W/m^2).

Meyer and Anderson (1952) analyzed that the proportion of energy used for photosynthesis and energy storage are from 3 to 8% and do not affect the energy balance in greenhouses significantly. Therefore, Some research that simulate the energy equation of plants in the greenhouse also did not consider the photosynthesis and thermal energy storage (Walker, 1965; Stanghellini, 1987; Luo et al., 2005; Demrati et al., 2007).

Sensible heat flux is the energy flow caused by the difference in temperature between the surface of the leaf and ambient air. For latent heat flux, the energy flow is caused by transpiration at the surface of the leaf. Contrary to sensible heat, latent

heat is affected not only ambient temperature, but also other environmental conditions such as the temperature of the leaf surface, solar radiation, carbon dioxide concentration, humidity. Plant transpiration is directly related to irrigation; therefore, physically and empirically based models that predict evapotranspiration (ET) have been developed by several researchers (Prenger et al., 2002). Penman (1948) developed the ET model for field cultivation crops based on the energy and mass balance equation. The water vapor transfer from an open water surface is analyzed thermodynamically and semi-empirically. The model suggests that the potential ET rate, which is measured from a well-watered reference crop (alfalfa), and the ET of a specific crop could be calculated by multiplying the potential ET and crop coefficient. The crop coefficient is the ratio of ET observed for the specific crop over the ET observed for the well calibrated reference crop under the same conditions. This differs by species and the plant's growing stage. As the potential ET was measured for a single species, the model cannot consider the density and height of specific crops. Monteith (1965) and Rijtema (1965) modified the Penman equation by considering ET from a specific condition such as species of crops, ground surface type rather than from a standard crop. They considered characteristic resistances of water transfer on plant surface, which change depending on plant species and shape, to rectify the ET calculating equation. The characteristic resistances to water vapor transfer at the canopy surface are divided into external and internal, however, Penman (1948) only considered the aerodynamics resistance for entire colony. The external resistance to vapor movement is from the surface of the leaf to the surrounding air while the internal resistance to vapor movement is from the leaf tissue to the surface of the leaf. The external resistance is affected by the boundary layer characteristics, such as wind velocity on the plant surface, while internal resistance changes according to characteristics of the leaf cuticle layer and the stomata. To improve the ET from plants, Monteith (1965) and Rijtema (1965) revised the plant ET model by considering the internal and external resistance more specific.

They defined the resistance assuming a fully develops, one-dimensional layer. Stanghellini (1987) revised the Penman-Monteith ET model to represent conditions in a greenhouse where air velocities are typically less than 1.0 m/s. The model includes more complex equations to calculate internal and external resistance. To apply the model in a greenhouse environment, Stanghellini (1987) focused on the energy exchange from the leaf and expanded it to the whole plant. The radiation absorption at multi-layers of the canopy is also considered by applying the leaf area index (LAI). Fynn (1993) also revised the Penman-Monteith ET model to predict the ET from crops in a greenhouse. However, Fynn (1993) assumed that solar radiation equals the crop height and used the canopy area index (CAI) to consider solar absorption by cultivation area. As the solar radiation which absorbed to plants are assumed to be equal by layer of plants, the latent heat flux of the plant should be overrated.

3. Materials and Methods

3.1. Target greenhouse

The target greenhouse is located on the west coast of South Korea in Boryeong city, which is 1 km south of the Boryeong thermal power plant (Fig. 2). The target greenhouse has 8 spans that are 34.2 m width, 30.0 m length, 5.7 m ridge height and 4.5 m eave height, and is covered with a single layer polyolefin film (0.15 mm thickness). The greenhouse is divided into a plant growth room (768 m^2 floor area) for the crop plantation and a workroom for mechanical control (128 m^2 floor area) (Fig. 3 and Fig. 4). The additional cladding is covered on the outside of the side wall so that an air layer can act as insulation.

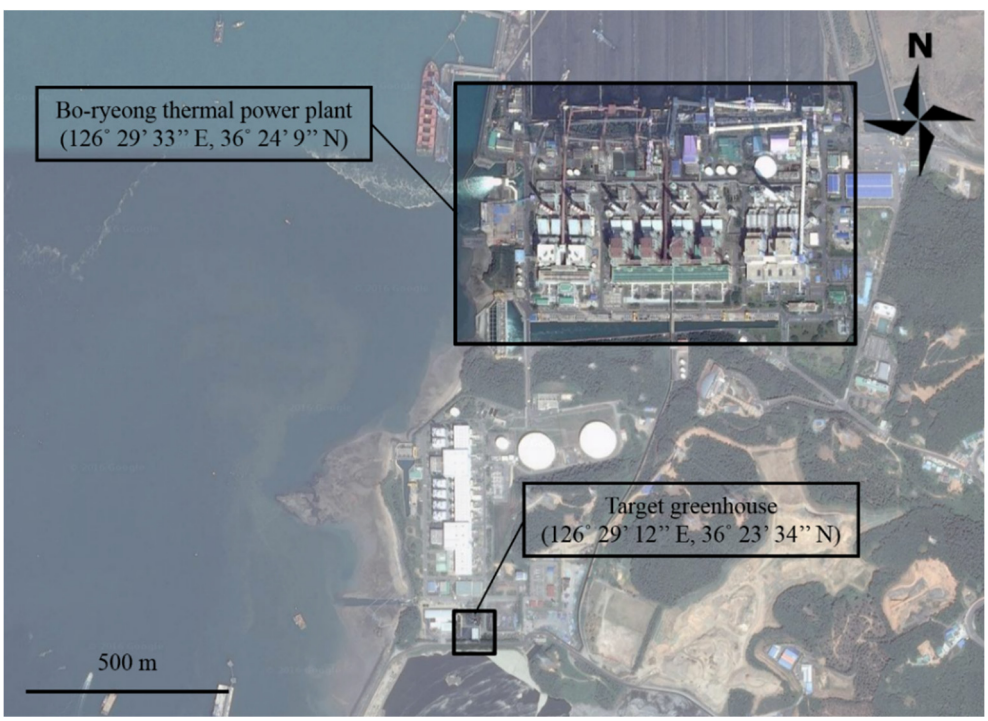

Fig. 2 Geographic information of the Boryeong thermal power plant and the target greenhouse

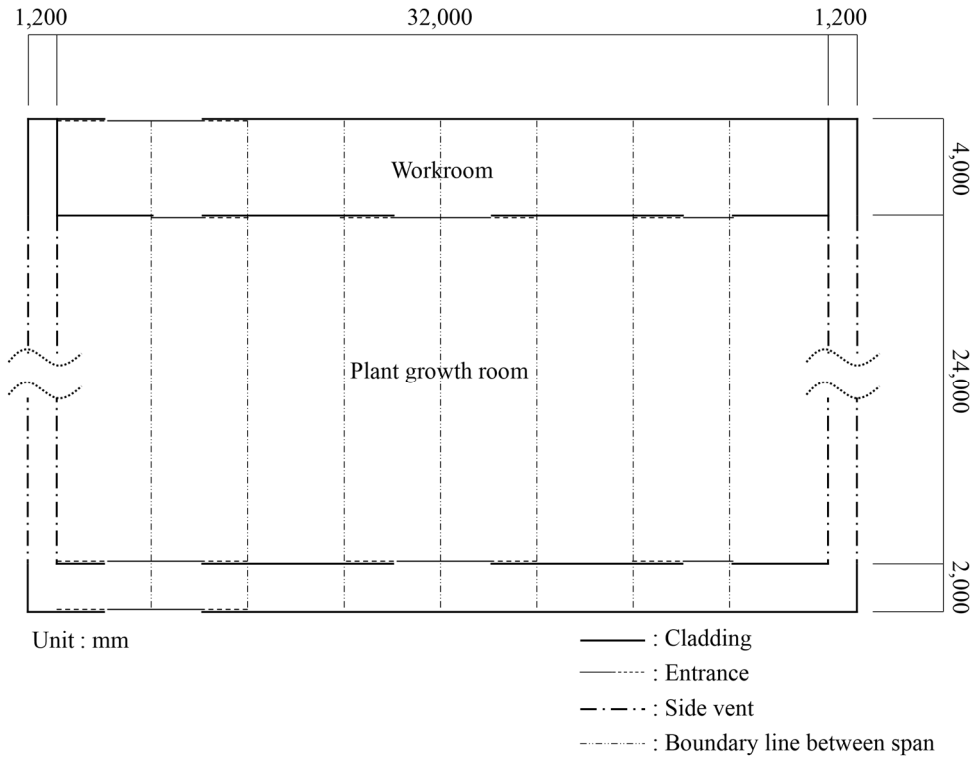

Fig. 3 Design drawing and space partition of the target greenhouse (top view)

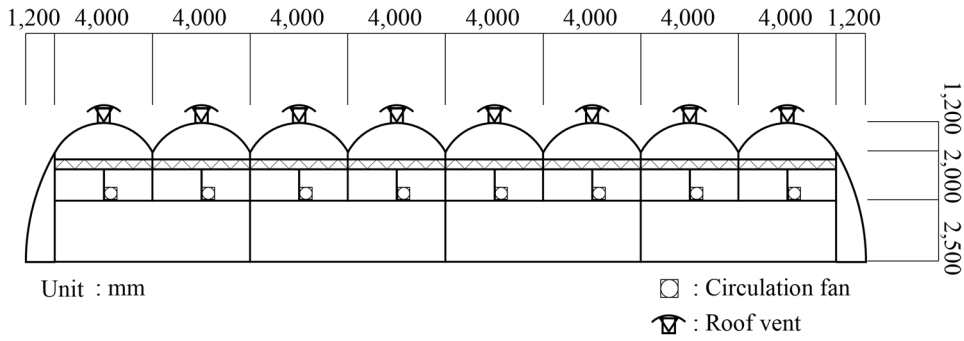

Fig. 4 Design drawing and structural characteristics of the target greenhouse (front view)

The greenhouse is occupied with 100 potted Irwin mango fruit trees. The Irwin mango is a dicotyledonous plant, which was developed in South Florida in 1939 to improve taste and flavor. The trees generally grow to a height of about 7 m if unpruned in an open field. The optimum growth temperature of the Irwin mango is usually over 20 ℃. However, to bear fruit, the plants have to be stressed by lowering the growth temperature under 20 ℃ for two months. In the target greenhouse, mango trees are pruned at around a 1.5 m height and the branches are pulled as a globular shape to equalize the light-interception. Therefore, mango trees in the greenhouse are fixed in shape and size during experimental periods (Fig. 5).

Fig. 5 Potted cultivation of Irwin mango in the target greenhouse

The target greenhouse was constructed to enhance the energy efficiency of heating and cooling system by utilizing a thermal effluent on a trial basis. The thermal effluent from the Boryeong power plant was used as a heat source for operating the heat pump. The Boryeong power plant is a power production facility, which is composed of 8 fuel generators (8 × 500 MW) and 9 combined fuel generators (9 × 150 MW). The facility discharges thermal effluent at around 3 billion

tons per year. The thermal effluent is stored initially in a water storage tank and then utilized on the farm and the greenhouse (Fig. 6).

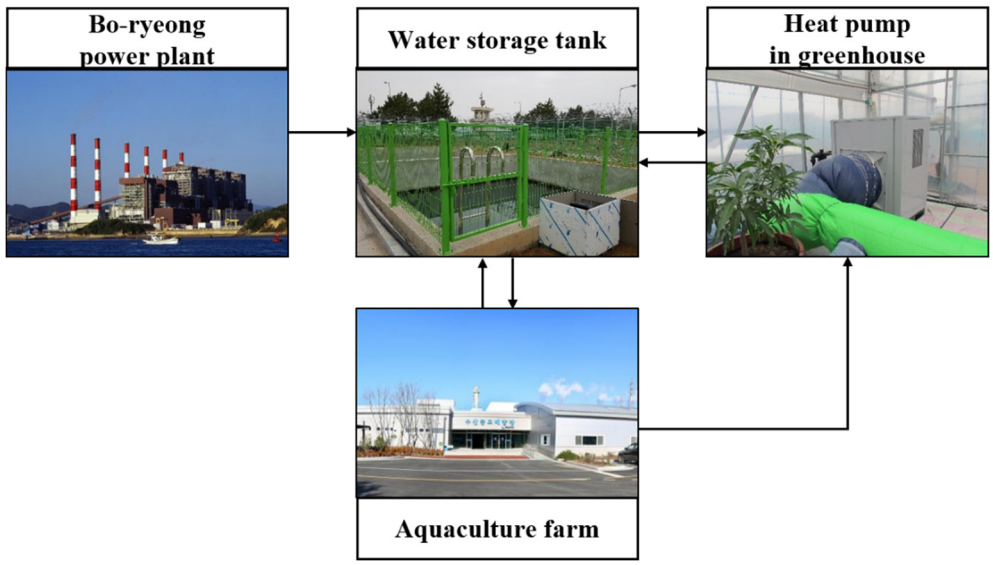

Fig. 6 Process of utilizing thermal effluent from the Boryeong thermal power plant to improve energy efficiency in the target greenhouse

The HVAC system is used for a proper growing environment and is composed of natural ventilation, and heating and cooling by a heat pump. The equipment is controlled automatically based on the inside air temperature and outside solar radiation. Natural ventilation is performed by a side vent and top vent. The side vent is located on the sidewall within a range of 0.5 m to 2.1 m and 2.7 m to 3.5 m from the bottom floor. The top vent is 0.6 m width and opened vertically, and is located on the ridge top of each span (Fig. 7).

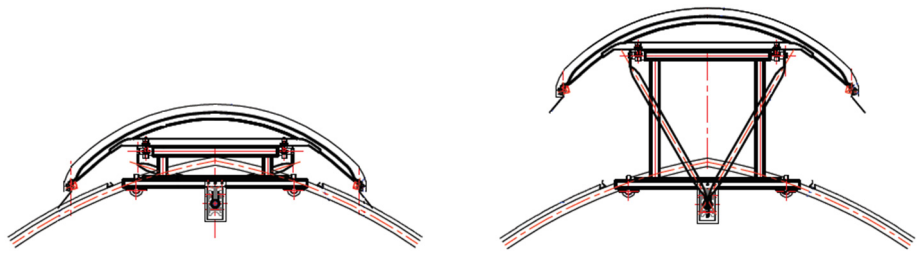

(a) Closed vent (b) Open vent

Fig. 7 Structural change when the top vent is operating

Thermal effluent from the power plant flow into the heat pump (ADF-SLX12WHB; Asan Co., South Korea) and is used to transfer or absorb heat from the greenhouse by an air blower, which is included in the heat pump. The performance of the heat pump is 43,276 W in maximum cooling capacity and 36,786 in maximum heating capacity. A total of three heat pumps are installed inside the plant growth room at both ends and center of the sidewall adjacent to the workroom. To supply heat energy uniformly, the air duct and circulation fan are installed in the greenhouse (Fig. 8). The air duct (60 cm diameter) is connected to the heat pump and the sub-air duct (40 cm diameter) is located between the pots. On the surface of the small air duct, holes with 6.5 cm diameter are bored at regular horizontal direction intervals of 1 m on both sides. 16 circulation fans (SGA-300P, Shinan Green Tech Co., South Korea) with a capacity of 35 m^3/min per unit are installed at a height of 2.5 m above the ground floor.

(a) Distribution of air duct

(b) Circulation fan

(c) Air blower of heat pump

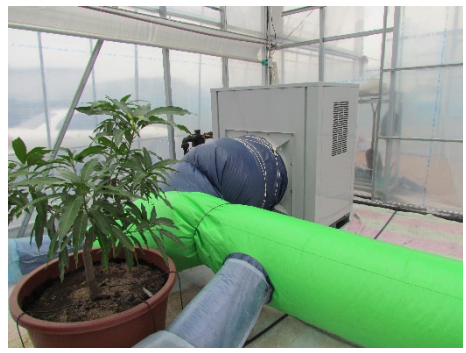

(d) Link between heat pumps and air duct

Fig. 8 Installation of heat pump, air duct, and circulation fan to improve the uniformity of conditioned air in the target greenhouse

Thermal screens are installed at the sidewall and ceiling to decrease conduction heat loss caused by temperature differences between the outdoor and indoor at the cladding. After sunset, the thermal screen at the sidewall is drawn vertically and the thermal screen at the ceiling is installed horizontally at a height of 3.8 m from the floor (Fig. 9).

(a) Vertical thermal screen (b) Horizontal thermal screen

Fig. 9 Installation of the thermal screen to decrease conduction heat loss through the cladding of the target greenhouse

3.2. Building energy simulation

Estimation of the energy loads is important for designing the building and enhancing the efficiency of energy usage. The calculating method for estimating energy loads is divided into the steady analysis method and a dynamic analysis method, according to a time factor. As mentioned in the literature review, the target structure of this study is a greenhouse that sensitive to a change in environmental conditions because of the thin cladding and plants. Therefore, in this study, the energy loads of the greenhouse are calculated by a dynamic analysis method.

To calculate the energy loads of the greenhouse by a dynamic analysis method, energy exchange in the greenhouse should be simulated by considering the environmental conditions, which changes over time. The BES technique, which analyzes energy exchange numerically in the building, is used to design the greenhouse energy exchange model. In agriculture, the BES technique is mainly used to assess the overall performance of various HVAC systems during the planning stage because of its high accuracy and usability. The BES technique is also used for the purpose of designing the heating and cooling system in the building, and efficiency analysis of newly utilized renewable energy such as solar energy, geothermal heat, and waste heat. To use this technique in diverse situations, various commercial dynamic BES programs have developed such as BLAST, DOE-2, EnergyPlus, ESP-r, eQuest, and TRNSYS. Among these programs, TRNSYS is a module-based program, which consist of the main program and several sub-routines to analyze energy flow of each component. TRNSYS also has the virtue of availability and compatibility on an enormous energy system because of a number of sub-routines which can compose various system such as heat pump, heat exchanger, solar collector, storage tank and can link each other. For instance, to compose the water circulation in heat pump system, the pipe component takes a water temperature and flow rate as an input data from data reader component and

calculate the water temperature and flow rate at the entrance of heat pump. Then, heat pump component uses the data from pipe component to calculate the energy production and power consumption which can used to estimate energy cost of building and energy supply in building component. To calculate the energy flow of the building, type 56 is mainly used to design the building system. Type 56 use a real-time weather data such as ambient air temperature, solar radiation, humidity, wind velocity as an input data and calculate the conductive and radiative energy exchange on each wall surface and convective energy exchange from ventilation and infiltration. The energy exchange inside the building are also considered as cooling and heating equipment and internal gains such as persons, electrical devices, and plants. By considering all these energy exchange elements, type 56 simulates radiation exchange and heat storage on the inside and outside wall dynamically and analyze the energy balance equation by time based on the transfer function method. The output data such as temperature of each wall, internal air enthalpy, the amount of energy exchange by each element can be acquired as text file. Therefore, energy flow of building in a specific time period can be simulated and the maximum or minimum value can be computed by TRNSYS (Fig. 10).

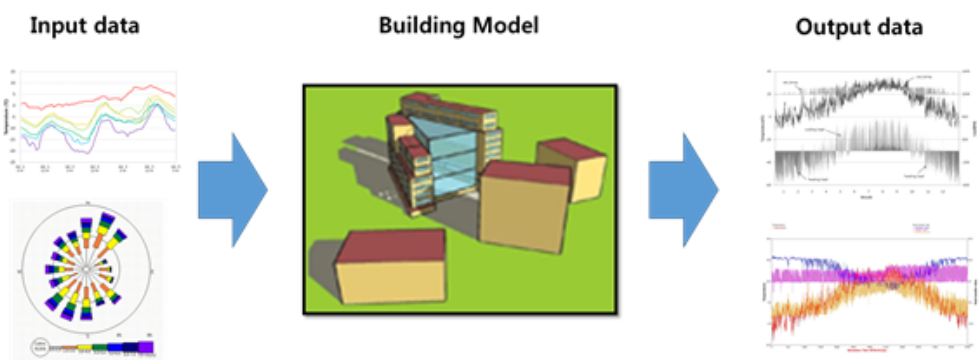

Fig. 10 Illustrative model of the energy exchange model for calculating energy loads using BES (Park, 2015)

The target building component in TRNSYS consists of several zones. The energy balance equation is analyzed by zone to simulate the thermal behavior for each zone. The zone is the domain that analyzes the energy exchange considering conduction, radiation, internal heat source, ventilation and infiltration based on the thermal capacity, density, and thermal conductivity of each wall. The adjacent zones also exchange the conductive and convective energy at each time step (Fig. 11, Eq. 2).

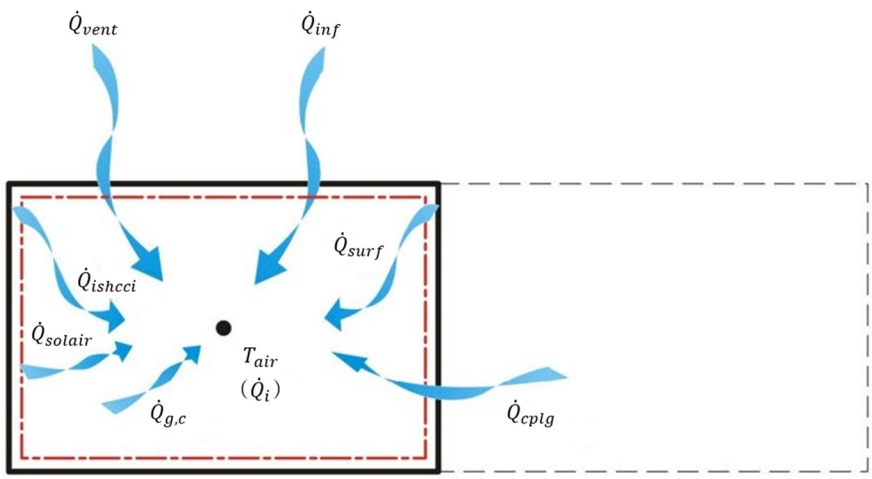

Fig. 11 Heat balance on the zone in TRNSYS

$$\dot{Q}_{surf} + \dot{Q}_{inf} + \dot{Q}_{vent} + \dot{Q}_{ishcci} + \dot{Q}_{solair} + \dot{Q}_{g,c} + \dot{Q}_{cplg} = \dot{Q}_i \quad \text{Eq. 2}$$

Where, $\dot{Q}_{surf}$ is a convective gain from surfaces (kJ), $\dot{Q}_{inf}$ is a infiltration gains (air flow from outside only, kJ), $\dot{Q}_{vent}$ is a ventilation gains (air flow from a user-defined source like an HVAC system, kJ), $\dot{Q}_{ishcci}$ is a absorbed solar radiation on all internal shading devices of zone and directly transferred as a convective gain to the internal air (kJ), $\dot{Q}_{solair}$ is a fraction of solar radiation entering a zone through

external windows which are immediately transferred as a convective gain to the internal air (kJ), $\dot{Q}_{g,c}$ is an internal convective gains (by people, equipment, illumination, radiators, etc., kJ), and $\dot{Q}_{cplg}$ is a gains due to (connective) air flow from adjacent zone or boundary condition (kJ).

3.3. Crop energy exchange model

To model the energy exchange by crops, energy exchange at the surface of the leaf should be analyzed firstly, then multiply the LAI to calculate the sensible and latent heat flux from entire canopy (Stanghellini, 1987). When solar radiation reaches the surface of the leaf, energy is partly dissipated by sensible heat, latent heat and partly stored in the leaf by photosynthesis and thermal energy. As mentioned in the literature review, the photosynthesis rate is a small proportion, therefore, the sensible heat, latent heat, and thermal energy were considered to model the crop energy exchange model (Eq. 3).

$$R_n = H + LE + J \qquad \text{Eq. 3}$$

The sensible heat can be calculated by the density, specific heat of air and ambient temperature which varies from the distance from the surface of the leaf (Eq. 4).

$$H(z) = -D' \frac{d\left(\rho_a, c_p, T_a(z)\right)}{dz} \qquad \text{Eq. 4}$$

Where, $H(z)$ is a sensible heat flux at height z (W/m^2), D' is a coefficient of diffusivity (m^2/s), ρ_a is a density of air (kg/m^3), c_p is a specific heat of air at constant pressure (J/kg·K), and $T_a(z)$ is a ambient temperature at height z (K).

However, ambient temperature at height z cannot be defined precisely because the profile of ambient temperature by distance from leaf surface is hard to measure. Moreover, an energy exchange between the entire leaf and the surrounding bulk air is dominant over the energy exchange between the surface of the leaf and the ambient

air of leaf surface. Therefore, the temperature difference between the leaf and surrounding bulk air can include temperature differences by distance from the leaf surface. As supposing that temperature of the air is constant according to the distance from the surface of the leaf, the external resistance of the surface of the leaf can be defined as a ratio of the diffusivity coefficient to the thickness of the surrounding air (Eq. 5).

$$H = \frac{\rho_a c_p}{r_e}(T_L - T_a) \qquad \text{Eq. 5}$$

Where, T_L is a temperature at the surface of the leaf (K), T_a is a ambient air temperature (K), and r_e is an external resistance of the surface of the leaf to sensible heat transfer (s/m).

When vapor pressure of the surface of the leaf and ambient air are different, plants start to transpire. Latent heat is the heat flux which is caused by transpiration (Eq. 6).

$$LE = \frac{\rho_a c_p}{\gamma r_{aV}}(e_L - e_a) \qquad \text{Eq. 6}$$

Where, γ is a thermodynamic psychometric constant (Pa/K), r_{aV} is a boundary layer resistance to vapor transfer (s/m), e_L is a vapor pressure at the surface of the leaf (Pa), and e_a is a vapor pressure of the air (Pa).

The vapor pressure at the external air layer of the leaf is equal to the vapor pressure at the surface of the leaf. To consider vapor transport from inside the leaf to ambient air, the resistance to vapor flow in the tissue layer of the leaf was calculated (Eq. 7).

$$LE = \frac{\rho_a c_p}{\gamma(r_{aV} + r_{iV})}(e_E - e_a) \qquad \text{Eq. 7}$$

Where, e_E is a vapor pressure at the external air layer of the leaf (Pa), and r_{iV} is a resistance to vapor flow in the tissue layer of the leaf (s/m).

The vapor pressure at the external air layer of the leaf can be assumed saturated because the surface of the leaf is composed of plant tissue. Therefore, the vapor pressure at the external air layer of the leaf can be calculated based on the correlation of saturated vapor pressure and air temperature (Eq. 8).

$$e_E = e^*(T_E) = e^*(T_a) + \delta(T_E - T_a) \qquad \text{Eq. 8}$$

Where, $e^*(T)$ is a saturation vapor pressure at temperature T (Pa), δ is a slope of the saturation vapor pressure-temperature curve (Pa/K), and T_E is a temperature at the external air layer of the leaf (K).

After arranging the temperature difference $(T_E - T_a)$ as $(T_E - T_L) + (T_L - T_a)$, Eq. 9 is yielded by substituting Eq. 3 and Eq. 8 into Eq. 7.

$$LE = \frac{\delta r_e(R_n - J) + \rho_a c_p(e_a^* - e_a)}{\gamma(r_{aV} + r_{iV}) + \delta r_e} \qquad \text{Eq. 9}$$

The summation of boundary layer resistance to vapor transfer and resistance to vapor flow in the tissue layer of the leaf can be defined as stomatal resistance (r_s), which is the total resistance vapor transfer from the body of the leaf to the surrounding air. Thermal energy, which is stored in the plants (J), is very variable according to radiation. Related studies on this topic have been rarely conducted. In

this study, thermal energy, which is stored in the plants, were calculated as 15% of the net flux of radiation (Monteith, 1975; Fynn et al., 1993).

The elements consisting of Eq. 5 and Eq. 9, and can be classified as an environmental factor and plant characteristic factors. The density, specific heat of air, leaf temperature, ambient temperature, and radiation are included in the environmental factor, which can be conducted by field experiments. Plants characteristics such as LAI, external resistance, and stomatal resistance can differ by crop species. External resistance can be calculated experimentally using Eq. 3, excluding thermal energy, which is stored in the plants. In this study, an empirical formula by Stanghellini (1987) is used to calculate external resistance (Eq. 10).

$$r_e = \frac{1174 l^{0.5}}{(l|T_L - T_a| + 207u^2)^{0.25}} \qquad \text{Eq. 10}$$

Where, l is a characteristic leaf dimension (m), and u is a wind speed (m/s).

The stomatal resistance has a negative correlation with the stomatal opening, which is directly related to the transport of water vapor at the surface of the leaf. The minimum value and the variance of stomatal resistance are different depending on the species. Therefore, to simulate energy exchange by crops more precisely, stomatal resistance should be considered in accordance with crop species. Stanghellini (1987) suggested that stomatal resistance can be varied by the growing environment such as ambient air temperature, humidity, carbon dioxide concentration, and radiation even for the same species. To simulate stomatal resistance precisely based on the change of environmental conditions, it is important to monitor stomatal resistance by time. A monitoring sensor for measuring stomatal resistance can be attached to the surface of the leaf, which could be an error factor to the result value. Another way to consider stomatal resistance by time is to develop a regression equation that has a variable related to the surrounding environment.

Several studies found the relationship between an environmental factor and stomatal resistance, and figured out that the solar radiation is the main parameter to stomatal resistance (Jarvis, 1976; Avissar et al., 1985; Stanghellini, 1987; Demrati et al., 2007). As many factors are considered to derive the regression equation, the description of the equation can be increased. Demrati et al. (2007) figured out that when derive regression equation for stomatal resistance, only two factor including the solar radiation above the plants are sufficient to describe variations. Therefore, in this study, the solar radiation above the plants and the surface temperature of the leaf is considered to derive the regression equation of stomatal resistance.

3.4. Research method

A flowchart for designing a dynamic energy exchange model of a greenhouse and calculating the energy loads is illustrated in Fig. 12. The weather data of the target area were analyzed and field experiments were also conducted. to design an energy model of the greenhouse. Greenhouse structural characteristics such as the shape, cladding, HVAC system were investigated to design the greenhouse structure model and crops characteristics such as stomatal resistance, and LAI were measured to design the crop energy exchange model. The inside and outside micro-climates of the greenhouse, such as solar radiation, and ambient temperature were also monitored to validate the energy model. Experimentally measured transpiration rate of the plants and ambient air temperature inside the greenhouse were used to validate the energy exchange model of crop and entire greenhouse, respectively. The validated model was used to calculate the hourly energy loads based on weather data. Then, the periodic and maximum energy loads was calculated to assess the scale of heat pump in target greenhouse and analyze the impact of the energy exchange by crops when calculating the energy loads of greenhouse. Additionally, the comparative analysis was conducted to estimate the reduction of energy cost when using the thermal effluent – heat pump system compared to kerosene boiler.

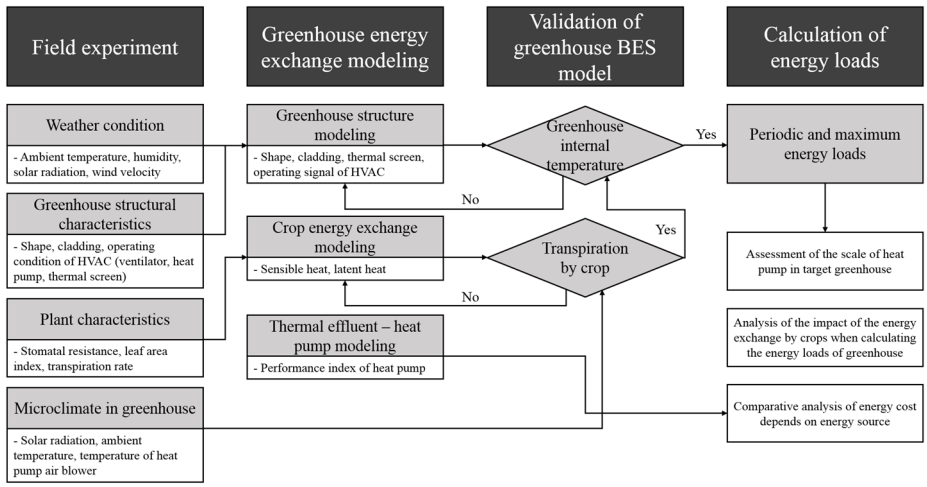

Fig. 12 Flow chart of this study

3.4.1. Field experiment

3.4.1.1. Micro-climate measurement in the greenhouse

The micro-climate was monitored to design and validate the greenhouse BES model (Fig. 13). To measure radiation transmissivity of the greenhouse cladding, a pyranometer (SP-110; Apogee Inst., USA) was installed on the center of top frame, which is 2.5 m above the bottom floor. The internal ambient temperature of the greenhouse was measured by a thermocouple (T-type; Ondo114 Co., South Korea), which is installed 1.0 m above the bottom floor. 15 thermocouples were installed to calculate the average ambient air temperature and 3 thermocouples were installed at the center of the air blower of each heat pump to monitor operating time of heat pump during experimental period. The installed sensors were connected to a data logger (GL 820; Graphtech Corp., USA) and the data was saved at five-second intervals.

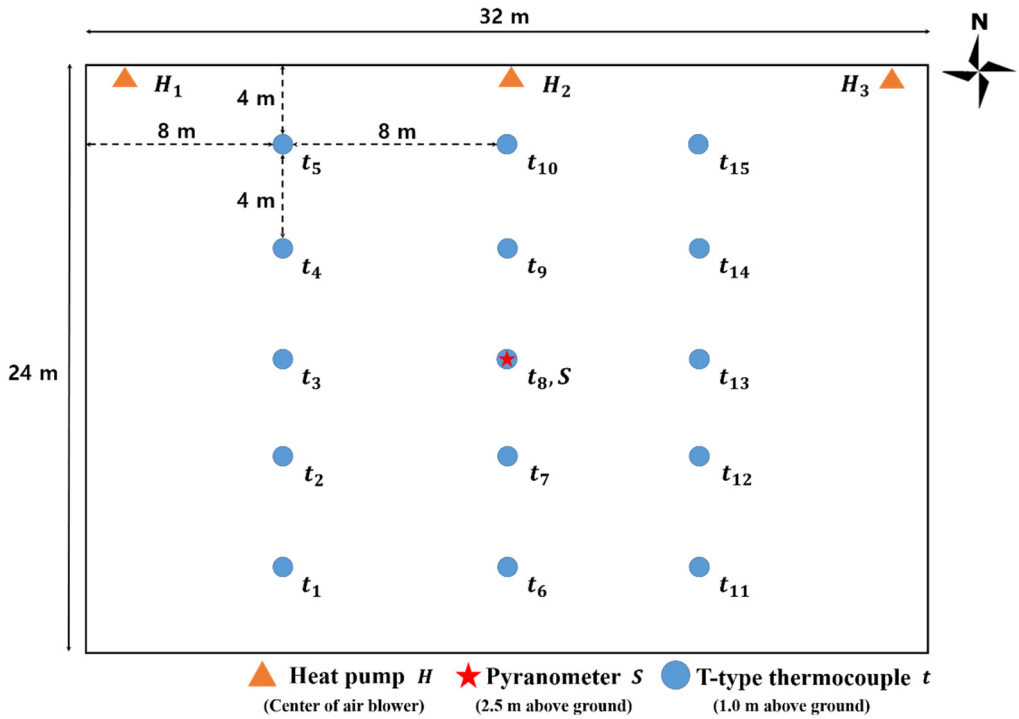

Fig. 13 Location of sensors for measuring the micro-climate in the target greenhouse (top view)

3.4.1.2. Measurement of stomatal resistance and leaf area index

Stomatal resistance and LAI of the Irwin mango in the greenhouse were measured to analyze plant characteristics. Data for regression analysis and radiation above the plants, which is the main factor of the regression equation, was also measured. In addition, surface temperature of the leaf and humidity surrounding crops are measured to derive a regression equation of stomatal resistance (Boulard et al., 1991). Among the several studies that derived a regression equation of stomatal resistance based on the same process, the equation used by Demrati et al. (2007) was applied in this study (Eq. 11, Eq. 12, Eq. 13, and Eq. 14). Demrati et al. (2007)

modeled leaf stomatal resistance of a banana crop cultivated in a greenhouse, which is the woody plant crops cultivated in a greenhouse.

$$r_s = r_{min} \cdot f_1(R_G) \cdot f_2(x_2) \quad \text{Eq. 11}$$

$$f_1(R_G) = 1 + \left[exp\left(a_1 \cdot (R_G - b_1)\right)\right]^{-1} \quad \text{Eq. 12}$$

$$f_2(D_{sat}) = 1 + a_2 \cdot exp\left(b_2 \cdot (D_{sat} - D_{max})\right) \quad \text{Eq. 13}$$

$$f_2(T_f) = 1 + a_2 \cdot exp\left(b_2 \cdot \left(T_f - T_{f,max}\right)\right) \quad \text{Eq. 14}$$

Where, R_G is a solar radiation (W/m^2), D_{sat} is a vapor pressure deficit (Pa), D_{max} is a maximum vapor pressure deficit (Pa), T_f is a leaf temperature (K), $T_{f,max}$ is a maximum leaf temperature (K), and a, b is a constants.

In this study, the regression equation of stomatal resistance was derived by using two parameters, solar radiation and the leaf temperature. As the Irwin mango in the target greenhouse is a perennial plant, the stomatal resistances at the ventral and dorsal side of the top, middle, and bottom leaf of the crops was measured using a leaf porometer (SC-1; Decagon devices, USA) to consider the growth level (Fig. 14). A leaf porometer is a sensor that measures vapor conductivity per unit area and calculates stomatal resistance by the reciprocal of the vapor conductivity. The radiation above the plants was measured by a pyranometer and the surface temperature of the leaf was measured by installing a thermocouple on the ventral side of the leaf.

(a) Measurement of stomatal resistance | (b) Measurement of radiation above the plant | (c) Measurement of leaf temperature

Fig. 14 The installtion of sensor to measure stomatal resistance and the surface temperature of leaf surface and solar radiation above the plant

LAI is the ratio of whole leaf area to ground area covered by plants, which represents leaf distribution and density. LAI can be measured by two methods, the indirect method and direct method. By the indirect method, LAI can be calculated based on the Beer-Lambert law, which is the exponential relationship between absorbance and concentration of absorbing materials. According to the Beer-Lambert law, when light penetrates the plant canopy vertically, light intensity decreased following the exponential law. Radiation above and under the canopy are measured by a plant canopy analyzer (LAI-2200; LI-COR Inc., USA) to calculate the average LAI of the Irwin mango in the greenhouse. LAI of a single canopy was also measured by the direct method to compare with the average LAI. To measure LAI in a nondestructive way, an empirical formula, which is derived by Jung et al. (2016) to calculate the leaf area of the Irwin mango based on leaf width and length (Eq. 15), was used.

$$LA = -14.623 + 8.074W + 0.085L^2 + 0.452W^2 \quad \text{Eq. 15}$$

Where, LA is a leaf area (cm^2), W is a leaf width (cm), and L is a leaf length (cm).

3.4.1.3. Measurement of transpiration by crops

The transpiration rate of the Irwin mango was measured to validate the energy exchange model of the crop. Transpiration is directly related to latent heat and therefore can be used as data for validation (Eq. 16).

$$E = \frac{LE}{\lambda} \qquad \text{Eq. 16}$$

Where, E is a transpiration per area (kg/s·m^2). LE is a latent heat flux (W/m^2), and λ is a latent heat of vaporization of water (J/kg).

To validate the energy exchange model of the crop, the transpiration rate of the target plant has to be calculated and then compared with the measured transpiration rate. The ambient air temperature, humidity, surface temperature of the leaf, stomatal resistance, and LAI were measured to calculate the transpiration rate (Fig. 15).

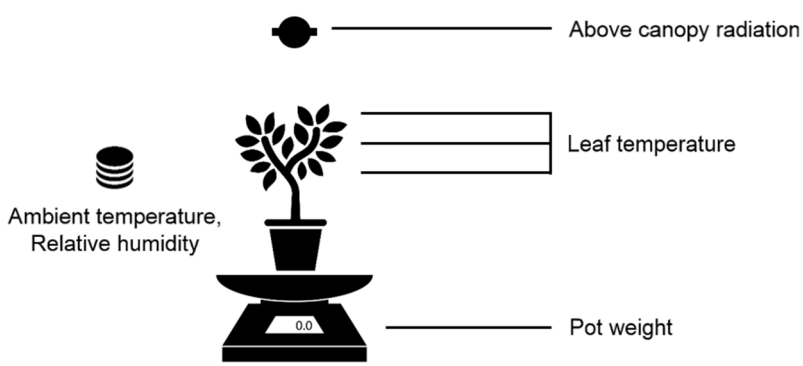

Fig. 15 Diagram for measuring the transpiration rate

The target plant is a three-year-old Irwin mango that is cultivated in a 44.5 cm diameter pot. The pot was placed on an electronic scale (CBX32KH; CAS Corp., South Korea) to measure the change in the weight of the pot by time. The weight of

the pot was recorded at five-minute intervals, excluding the watering periods. To exclude water evaporation from the soil and to measure only transpiration from the plant, the soil part of the pot was sealed with plastic wrap. A pyranometer was installed on the center of the top frame to measure radiation and 3 thermocouples were installed on the dorsal side of the leaf (i.e., top, middle, and bottom) to measure the surface temperature of the leaf. Three HOBO data loggers (UX100-003; Onset Corp., USA) were also installed near the plant to measure ambient temperature and humidity. Fig. 15 is a diagram of this experiment to measure the transpiration rate. Fig. 16 is the composition of the experiment equipment to measure the transpiration rate. The Irwin mango received 1 liter of water at 9:00 PM so that the plant can transpire sufficiently.

(a) Overall experiment equipment

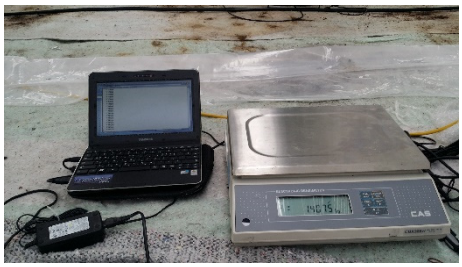

(b) Electronic scale and computer for measuring change in the weight of the pot

(c) Plastic wrap for sealing the pot to prevent evaporation from the soil

(d) Pyranometer used for measuring radiation above the plant

Fig. 16 Composition of the experiment equipment for measuring the transpiration rate of the Irwin mango

3.4.2. Design method of the greenhouse energy exchange model by BES

A dynamic energy exchange model of the greenhouse was designed by adapting three model: greenhouse structure modeling, crop energy exchange modeling, and thermal effluent – heat pump modeling. As energy exchange by radiation and conduction at cladding is varied by shape and materials of the greenhouse, it is important to model greenhouse cladding precisely. A curved surface of the roof and sidewall of the target are modeled by using TRNSYS3D plugin and Google SketchUp (ver.8, Google, USA). As the TRNSYS program is optimized for modeling a thick wall of a general building, there is some limitations to model the cladding of a greenhouse using TRNSYS. In this study, the method to model the greenhouse cladding was conducted based on Ha et al. (2016) methodology. The cladding was realized as a window in type56 of TRNSYS while considering the frame rate and optical properties of the cladding. There are no data for modeling polyolefin film in standard window library of TRNSYS. Thus, WINDOW program (ver.7.4, LBNL, USA) was used to realize the cladding material of the greenhouse.

Inside the target greenhouse, a heat pump and ventilator were operated according to the internal ambient temperature and thermal screen was operated according to time. The operating condition for all equipment was measured by a field experiment and input as a boundary condition in the greenhouse BES model. The environmental conditions and characteristics of plants are used to model the energy exchange model of the crop based on Eq. 5 and Eq. 9. Real time greenhouse internal micro-climate data are used to validate the energy exchange model of the crop. However, when calculating greenhouse energy loads in the past, there is a limitation in simulating the energy exchange of the crop because of the absence of real time greenhouse internal micro-climate data. Therefore, the ratio of sensible and latent heat to external radiation was analyzed to simulate the greenhouse BES model based

on research by Al-Helal and Abdel-Ghany (2011) research. Al-Helal and Abdel-Ghany (2011) figured out that the specific ratio between the energy exchange by plants and the external radiation depend on the species and density of the plants. The ratio of sensible and latent heat from plants to the external radiation was derived from the validated the energy exchange model of the crop in this study. The thermal effluent – heat pump system was modeled based on performance data of the heat pump. Discharge flow data of the thermal effluent were used to calculate the energy production and power consumption by the heat pump per unit of time. Several components in TRNSYS such as data reader to read weather data as a input, psychometric equation to calculate the properties of moist air, online plotter to record the energy flow inside the greenhouse were used to model each part (Table 1).

Table 1 Description of components for modeling the target greenhouse

	Components	Specification
	Data reader - weather station data, sensor data	Reads weather and sensor data to send input data to other components
	Radiation processor	Interpolates radiation data; calculates several quantities related to the position of the sun and estimates insolation on a number of surfaces of either fixed or variable orientation
	Psychometric	Calculates moist air by taking input dry bulb temperature and relative humidity
	Sky temperature calculator	Determines effective sky temperature to calculate the long-wave radiation exchange between an arbitrary external surface and the atmosphere
	Multi-zone building (greenhouse)	Models the thermal behavior inside a greenhouse (e.i., heating, cooling, ventilation, and infiltration)
	Online plotter	Displays and records selected system variables while the simulation is in process
	User defined function	Calculates average greenhouse internal temperature as input data for the switch component; sensible/latent heat flux by crops; and energy production and power consumption of the heat pump
	Switch	Determines on/off signals to each device based on the external/internal weather conditions
	Water source heat pump	Models single-stage liquid source heat pump based on user-supplied data files containing catalog data for the capacity and power

3.4.3. Validation method of the greenhouse BES model

To validate the dynamic energy exchange model of greenhouse, several researchers evaluate their model quantitatively and qualitatively by using the statistics index and tendency (Luo et al., 2005; Sethi 2009; Candy et al., 2012; Fatnassi et al., 2013; Chen et al., 2015). As the energy model of greenhouse is composed of several elements such as cladding, soil, solar collector, heat exchanger, to evaluate the accuracy of the model more precisely, many researchers validated

their model for two steps, the entire energy model and each component in greenhouse (Du et al., 2012; Mashonjowa et al., 2013; Ntinas et al., 2014; Attar et al., 2015; Joudi et al., 2015). Designed BES model computed air temperature inside the greenhouse, which was simulated using measured indoor and outdoor environment data, was compared with measured internal air temperature to validate the greenhouse BES model. The transpiration rate was simulated based on Eq. 5 and Eq. 9 was also compared with the measured transpiration rate to validate the energy exchange model of the crop. The measured crop characteristics and environmental conditions such as LAI, ambient air temperature, humidity, radiation above plants were used to simulate the transpiration rate.

In this study, the coefficient of determination (R^2) was used to analyze the tendency. The index of agreement (d) was used to assess the error between simulated data and measured data. R^2 is the coefficient that only indicates the tendency between two groups of data, not direction or errors. R^2 can take on a value between '0' to '1'. The two groups of data have similar tendencies as R^2 becomes closer to 1 (Eq. 17). The index of agreement can standardize the measure of the degree of model prediction error, which can take on a value between '0' to '1'. As the index gets closer to 1, the simulated data correspond with the measured data (Eq. 18).

$$R^2 = \frac{\sum_i^n \left(Y_{i|mea} - \overline{Y_{mea}}\right)\left(Y_{i|sim} - \overline{Y_{sim}}\right)^2}{\sum_i^n \left(Y_{i|mea} - \overline{Y_{mea}}\right)^2 \sum_i^n \left(Y_{i|sim} - \overline{Y_{sim}}\right)^2} \qquad \text{Eq. 17}$$

$$d = \frac{\sum_i^n \left(Y_{i|mea} - Y_{i|sim}\right)^2}{\sum_i^n \left(\left|Y_{i|sim} - \overline{Y_{mea}}\right| + \left|Y_{i|mea} - \overline{Y_{mea}}\right|\right)^2} \qquad \text{Eq. 18}$$

Where, n is a number of measurement, $Y_{i|\mathrm{mea}}$ is a i[th] measured data, $Y_{i|sim}$ is a i[th] simulated data, $\overline{Y_{mea}}$ is an average of measure data, and $\overline{Y_{sim}}$ is an average of simulated data.

3.4.4. Calculation of greenhouse energy loads and prediction of energy cost

The target greenhouse maintains the growing environment in a proper range of temperatures for growing the plants. However, to bear fruit, the plants have to go through several growing stages, which have a diverse range of growing temperatures. The set temperature for heating, cooling and ventilation is set based on the optimum growing temperature for each growth stage (Table 2). To analyze the tendency of energy loads, 10 years of weather data (2006 to 2015) were used to calculate the energy loads of the greenhouse. Periodic and maximum energy loads are calculated by summarizing and comparing the hourly energy loads for each year. Based on the growth periods, the analysis period for each year started from the 1st of June through the 30th of May. As the Boryeong thermal power plant only provided five-year of discharge flow data, the temperature of thermal effluent and daily oil price for five-year (2010 to 2014) were used to compare the energy cost, which is dependent on the energy source.

Table 2 Optimum temperature according to the growth stage of Irwin mango

Stage	Period	Set temperature (℃)		
		Heating	Cooling	Ventilation
Vegetation	06/01 ~ 08/14	20	30	27
Floral-initiation	08/15 ~ 10/19	8	20	17
Flowering	10/20 ~ 12/31	18	25	22
Fruit-bearing	01/01 ~ 02/14	22	30	27
Fruit-growing	02/15 ~ 04/14	25	30	27
Harvesting	04/15 ~ 05/31	25	30	27

4. Results and Discussion

4.1. Results of field experimental data

4.1.1. Measured micro-climate features in the target greenhouse

Field experiment was conducted from 28th of May to 1st of June, 2016 to monitor the micro-climate features in the greenhouse. The internal ambient temperatures by location and time are analyzed according to day (8:00 AM to 8:00 PM) and night (8:00 PM to 8:00 AM) (Table 3). The average ambient temperature of the entire period is 29.9 ℃, and the standard deviation of each location is 0.57 ℃, which is quite low. The average ambient temperature and standard deviation for each location at day and night were found to be 33.6 and 25.4 ℃ and 0.92 and 0.30 ℃, respectively. The standard deviation of each location at night is lower than the during the day because air ducts and circulation fans are installed to ensure that the thermal environment of the plant growth room remains uniform.

Table 3 Average air temperature of each point for day and night (Unit: ℃)

Location	Average temperature	Average diurnal temperature	Average nocturnal temperature
t_1	29.5	33.3	25.0
t_2	29.4	33.1	25.1
t_3	29.8	33.5	25.4
t_4	29.6	33.3	25.2
t_5	29.3	33.1	24.8
t_6	30.2	34.2	25.5
t_7	30.0	33.6	25.7
t_8	29.3	32.5	25.5
t_9	29.2	32.6	25.2
t_{10}	29.6	33.3	25.4
t_{11}	31.1	35.5	25.9
t_{12}	30.5	34.4	25.9
t_{13}	29.3	32.5	25.7
t_{14}	30.5	34.8	25.5
t_{15}	30.4	34.8	25.2
Average	29.9	33.6	25.4
Standard deviation	0.57	0.92	0.30

Fig. 17 shows a graph of the average temperature at the center of three heat pump air blowers and the average internal air temperatures. As shown in the graph, the set temperature of the heat pump on the 28th, 29th, and 30th of May was 25 ℃ and the temperature of an air blast was approximately 42 ℃ when the heat pump is operated. However, on 27th of May, the heat pump did not work, and after the 31st of May, the set temperature of the heat pump was increased by approximately 2 ~ 3 ℃.

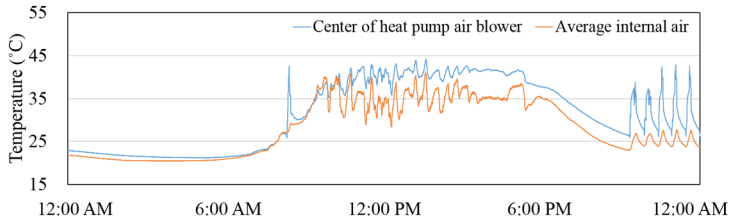

(a) 28th May 2016

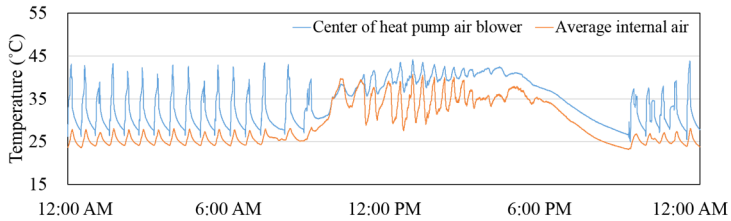

(b) 29th May 2016

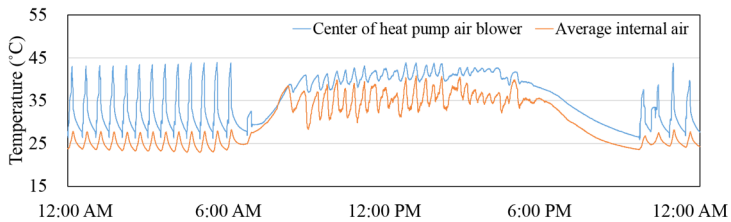

(c) 30th May 2016

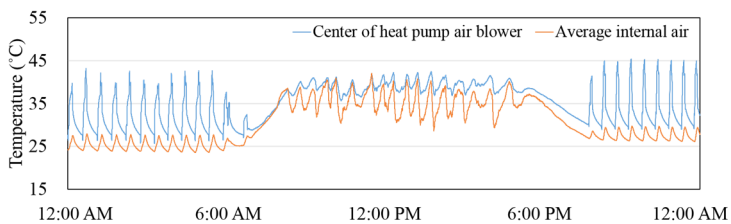

(d) 31st May 2016

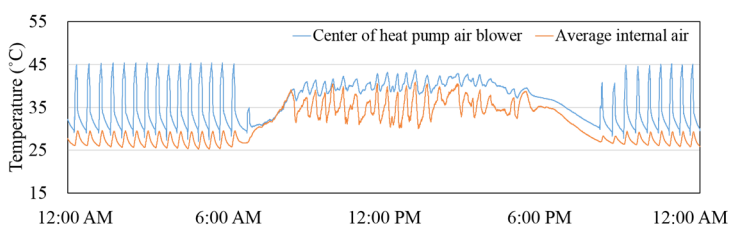

(e) 1st May 2016

Fig. 17 Temperature at the center of the heat pump air blower (28th May 2016 to 1st June 2016)

Fig. 18 is a graph which compares the solar radiation outside and inside the target greenhouse. The trend of the solar radiation inside the greenhouse usually follows that of the radiation outside; however, the solar radiation inside decreased at approximately 2:00 PM every day owing to shade from a folded thermal screen. The average radiation transmissivity of the cladding, except for the data at around 2:00 PM, was analyzed and found to be 83%.

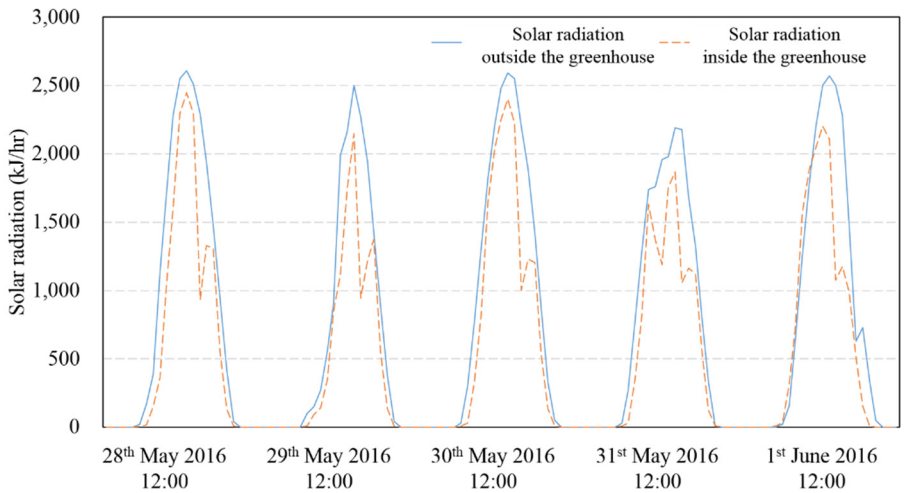

Fig. 18 Solar radiation outside and inside the target greenhouse (28th May 2016 to 1st June 2016)

4.1.2. Measured stomatal resistance and leaf area index of crops in cultivation

A field experiment to measure the stomatal resistance of the crops in the greenhouse was conducted on the 17th and 18th of May, 2016. The stomatal resistance and the leaf temperature at the ventral and dorsal sides of the top, middle, bottom leaf were measured 24 times, and parts of these results are listed in Table 4. The average stomatal resistance on both sides of the top, middle, bottom leaf was analyzed and the average value was found to differ depends on the side of the leaf. As Irwin mango is a perennial plant, the stomata are distributed on the ventral side of the leaf and scarcely exist on the dorsal leaf. For this reason, there were significantly fewer stomata on the dorsal side of the leaf than on the ventral side. The average stomatal resistance on the dorsal side (top leaf: 2,023 s/m, middle leaf: 1,820 s/m, bottom leaf: 1,906 s/m) was analyzed and found to be much higher than the average stomatal resistance on the ventral side (top leaf: 850 s/m, middle leaf: 168 s/m, bottom leaf: 264 s/m). Moreover, as the top leaves sprouted in less than one year, the stomatal resistances levels of the top leaf were least three additional times (3.22 ~ 5.06) as compared to the stomatal resistances levels of the middle and bottom leaves.

Table 4 Part of the experimentally measured stomatal resistance and leaf temperature of Irwin mango at the bottom, middle, and top leaf

	Time	Bottom leaf				Middle leaf				Top leaf (leaflets)			
		Stomatal resistance (s/m)		Leaf temperature (℃)		Stomatal resistance (s/m)		Leaf temperature (℃)		Stomatal resistance (s/m)		Leaf temperature (℃)	
		Ventral side	Dorsal side	Ventral side	Dorsal side	Ventral side	Dorsal side	Ventral side	Dorsal side	Ventral side	Dorsal side	Ventral side	Dorsal side
1	17th Feb. 2016 15:29	175		29.1									
	17th Feb. 2016 15:33		2,666		30.1								
	17th Feb. 2016 15:35					185		30.8					
	17th Feb. 2016 15:37						2,384		31.4				
	17th Feb. 2016 15:39									1,055		31.7	
	17th Feb. 2016 15:41										2,199		31.8
2	17th Feb. 2016 15:43	109		31.9									
	17th Feb. 2016 15:45		2,091		32.0								
	17th Feb. 2016 15:47					141		32.3					
	17th Feb. 2016 15:49						2,075		32.4				
	17th Feb. 2016 15:51									1,285		32.6	
	17th Feb. 2016 15:52										2,023		32.8
3	17th Feb. 2016 15:54	111		32.8									
	17th Feb. 2016 15:56		1,904		32.7								
	17th Feb. 2016 15:58					109		32.6					
	17th Feb. 2016 16:00						2,186		32.4				
	17th Feb. 2016 16:02									1,167		31.8	
	17th Feb. 2016 16:04										2,683		31.3

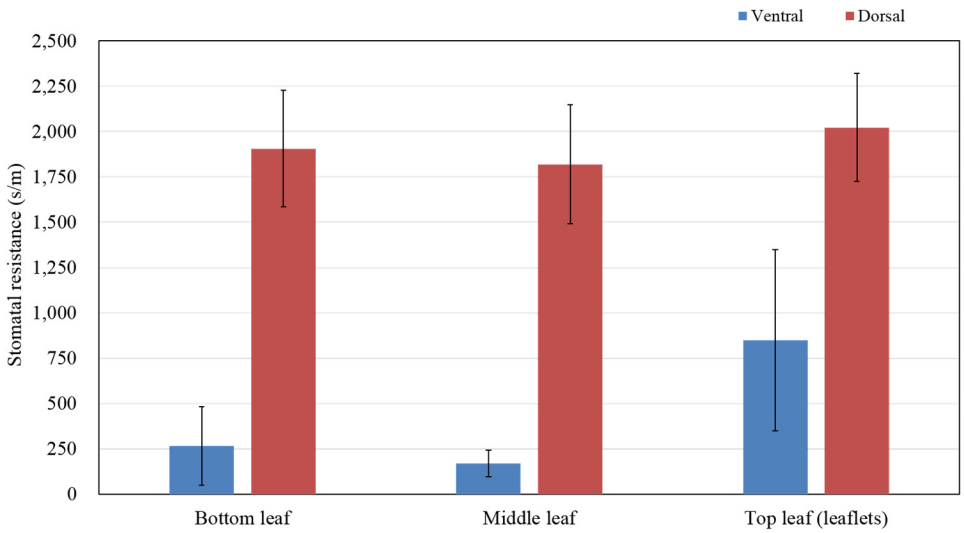

Fig. 19 Average stomatal resistance of irwin mango at ventral and dorsal surfaces

In this study, the stomatal resistance and leaf temperature on the ventral side of the middle and bottom leaves are used to derive a regression equation. Among 48 sets of stomatal resistance, radiation and leaf temperature data for the ventral side of the middle and bottom leaves, 38 set of data were used for the regression analysis, excluding outliers (Table 5). The SPSS program (Ver.23, IBM Corp., USA) was used to derive the non-linear regression equation for stomatal resistance.

Table 5 Stomatal resistance, radiation, and leaf temperature for the modeling regression equation of Irwin mango plants

Number	Stomatal resistance (s/m)	Radiation (W/m^2)	Leaf temperature (℃)
1	175	178.6	29.1
2	109	208.1	31.9
3	111	168.1	32.8
4	173	59.2	29.2
5	287	117.6	28.0
6	236	74.3	29.0
7	402	53.8	20.4
8	313	88.1	25.3
9	359	20.3	26.7

10	235	283.3	21.3
11	143	265.5	27.5
12	163	329.9	28.7
13	133	197.9	29.6
14	160	214.7	29.4
15	121	161.7	29.4
16	98	420.6	36.5
17	114	476.5	33.5
18	151	452.5	27.5
19	169	417.4	30.8
20	168	300.2	29.0
21	197	378.5	29.3
22	185	549.4	30.8
23	141	473.3	32.3
24	109	359.7	32.6
25	110	496.2	28.0
26	129	835.9	28.2
27	230	404.5	29.2
28	272	31.0	27.8
29	110	651.5	23.5
30	184	365.6	28.4
31	152	698.5	29.5
32	173	514.6	29.2
33	121	431.6	29.2
34	151	548.7	29.8
35	107	677.3	27.9
36	99	755.8	30.9
37	146	592.2	27.4
38	139	757.3	30.4

The minimum stomatal resistance and maximum leaf temperature were set to 98 s/m and 36.5 ℃, respectively, based on measured data. The regression equation was derived and used as a parameter for a plant energy exchange model (Eq. 19). The derived equation was found to be able to simulate the actual stomatal resistance precisely ($r = 0.85$, $d = 0.92$).

$$r_s = 98\left[1 + \{exp(0.011(R_G - 29.836))\}^{-1}\right] \left[1 + \left\{0.172exp\left(-0.127(T_f - 36.5)\right)\right\}\right] \quad \text{Eq. 19}$$

To calculate the average LAI of Irwin mango in the greenhouse, a plant canopy analyzer was used to measure LAI of 50 Irwin mango pots on the 17th of February and the 10th of April, 2016 (Fig. 20). The average LAI of these 50 crops was 1.81 and 1.76 in each case, respectively. The average value of 1.78 was used in the design of the plant energy exchange model.

Fig. 20 Measurement of leaf area index by an indirect method

The leaf width and leaf length were also measured to calculate the LAI directly. In total, 68 leaf areas were measured, with the outcome divided by the pot area to calculate the LAI (Table 6). The pot and total leaf areas were 1,555.28 and 3699.87 cm^2, respectively. Therefore, the LAI of the target crop was calculated and found to be 2.38. This value was used to validate the plant energy exchange model.

Table 6 Leaf width, length, and area used for calculating the leaf area index by an direct method

Number	Leaf width (cm)	Leaf length (cm)	Leaf area (cm^2)
1	4.7	18.5	62.4
2	3.5	16.0	40.9
3	4.0	18.0	52.5
4	7.0	24.0	113.0
5	5.0	16.0	58.8
6	4.6	19.0	62.8
7	3.2	15.0	35.0
8	4.0	19.0	55.6
9	3.5	16.0	40.9
10	3.5	18.0	46.7
11	2.5	14.0	25.1
12	3.5	18.0	46.7
13	3.0	16.0	35.4
14	3.5	19.0	49.9
15	2.5	14.0	25.1
16	2.5	13.5	23.9
17	3.0	12.0	25.9
18	3.5	14.0	35.8
19	4.0	19.0	55.6
20	4.2	21.0	64.8
21	3.0	14.0	30.3
22	3.0	14.0	30.3
23	3.6	17.0	44.9
24	4.0	20.0	58.9
25	5.0	21.0	74.5
26	5.1	26.0	95.8
27	4.1	21.0	63.6
28	4.8	21.0	72.0
29	3.5	18.0	46.7
30	4.0	21.0	62.4
31	4.5	19.0	61.6
32	4.2	20.0	61.3
33	4.3	20.0	62.5
34	5.6	23.0	89.7
35	5.1	24.0	87.3
36	5.0	22.0	78.2
37	5.0	23.0	82.0
38	5.0	22.0	78.2

39	4.0	18.0	52.5
40	4.0	15.0	44.0
41	3.5	17.0	43.7
42	4.8	20.0	68.6
43	4.5	20.0	64.9
44	4.5	20.5	66.6
45	3.8	20.0	56.6
46	4.0	19.0	55.6
47	4.2	20.0	61.3
48	2.8	15.0	30.7
49	5.0	22.0	78.2
50	4.0	19.0	55.6
51	4.0	18.0	52.5
52	3.8	16.0	44.4
53	3.7	16.0	43.2
54	4.2	20.0	61.3
55	4.2	21.0	64.8
56	4.2	22.0	68.4
57	4.0	19.0	55.6
58	3.6	19.0	51.0
59	4.0	20.0	58.9
60	3.5	19.0	49.9
61	3.9	19.0	54.4
62	3.7	20.0	55.4
63	2.7	14.0	27.1
64	3.3	18.0	44.5
65	3.5	18.0	46.7
66	3.0	16.0	35.4
67	3.5	18.0	46.7
68	2.5	14.0	25.1
Average	3.9	18.5	54.4

4.1.3. The change of transpiration by crops by time

The transpiration rate of the crops was measured over a time of 120 hours from the 28th of May to the 1st of June, 2016. The weight of the pot in each case was recorded at five-minute intervals, and 1,440 sets of data were saved in total (Fig. 21). During the daytime, the crops transpired actively, whereas during the nighttime (8:00 PM to 5:00 AM), the average measured transpiration rate was 0.535 g/crop. On the other hand, on the night of the 28th of May, the average transpiration rate was 0.154 g/crop, 70% lower than all nighttime periods of the experimental period. This result stemmed from the water content of the plants, which rose after the 28th of May in that irrigation provided one half of a liter of water, typically at 9:00 AM, while one a liter of water was provided by irrigation every evening at 9:00 PM during the experimental period. For the same reason, the average transpiration rate during the daytime (9:00 AM to 6:00 PM) on the 28th of May (7.212 g/crop) was found to be 15% lower than all daytime amounts during the experimental period (8.427 g/crop).

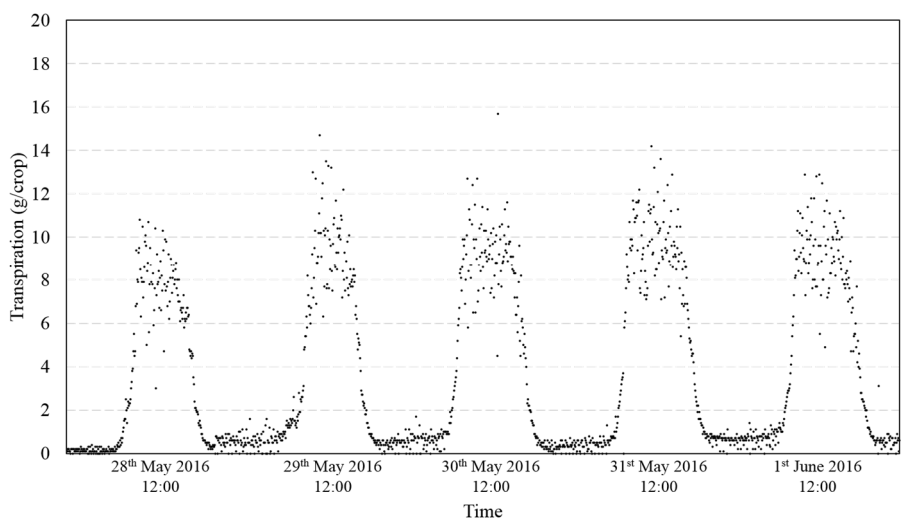

Fig. 21 Transpiration rates of the experimental poted plants (28th May 2016 to 1st June 2016)

4.2. Design of the greenhouse BES model

4.2.1. Greenhouse structure modeling

The structure of the target greenhouse was modeled based on a blueprint, and the width, ridge height and eave height were configured as 4.0, 5.7, and 4.5 m, respectively. As type56 cannot create the internal wall in single zone, the plant growth room was divided horizontally to set the thermal screen in the greenhouse. Each span was numbered from 1 to 8 from west to east. Fig. 22 shows the geometry of the greenhouse model except for the space on the south side of the plant growth room.

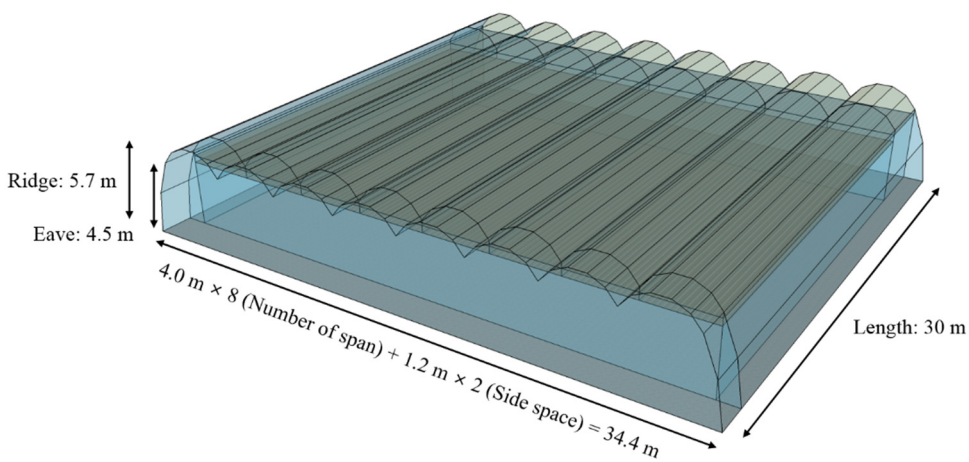

Fig. 22 Design showing the greenhouse dimensions and cladding

The physical properties of 0.15 mm polyolefin film were configured as follows: thermal conductivity of 0.330 W/m · K, solar transmittance of 0.797, solar reflectance of 0.106, visible transmittance of 0.935, visible reflectance of 0.106, thermal infrared transmittance of 0.000, and infrared emittance of 0.840. A single layer of polyolefin film was modeled based on these properties. As the cladding of the target greenhouse is a single layer, the window for the greenhouse cladding was

modeled as a single layer. The structure data and window data for the greenhouse model were exported from Google SketchUp and from the WINDOW program, respectively. Each span had an identical shape (24 m in length, 4 m in width, a 96 m^2 floor area and a volume of 509.96 m^3). The cladding was configured with the area set identically to that of the wall, except for the frame and imported window data. Carbon steel was used for the frame of the greenhouse and gravel and cotton were used on the floor (Table 7).

Table 7 Material properties by the wall type of greenhouse

Type	Material	Density (kg/m^3)	Specific heat (kJ/kg · K)	Thermal conductivity (kJ/h·m·K)	Thickness (m)
Framework	Carbon	7,840	0.502	154.8	0.0254
Floor	Gravel	1,800	1.000	7.2	0.2000
	Cotton	1,550	1.338	0.104	0.0100

Each zone was designed based on the properties of the wall and windows. To set the thermal screen, each span was divided into three zones; therefore, there were 24 zones for the plant growth room, two zones for the workroom and three zones for the area surrounding the plant growth room (Table 8). A virtual wall was set up between each span to simulate thermal exchange by convection and between the upper sides of the plant growth room to configure the thermal screen on the working schedule.

Table 8 The wall type, area, material, and adjacent zone of wall by each zone

Type	Area (m^2)	Specification		Bearing or adjacent zone
SPAN1				
Wall	15.20	PO film	ADJACENT	OUTZONE_BACK
Wall	15.20	PO film	ADJACENT	OUTZONE_FRONT1
Wall	91.20	PO film	ADJACENT	SIDE1
Wall	96.00	Virtual wall	ADJACENT	ROOF1_DOWN
Wall	91.20	Virtual wall (Thermal screen)	ADJACENT	SPAN2

Floor	96.00	Gravel	BOUNDARY	
ROOF1_DOWN				
Wall	1.60	PO film	ADJACENT	OUTZONE_BACK
Wall	1.60	PO film	ADJACENT	OUTZONE_FRONT1
Wall	9.60	PO film	ADJACENT	SIDE1
Wall	9.60	Virtual wall	ADJACENT	ROOF2_DOWN
Wall	96.00	Virtual wall (Thermal screen)	ADJACENT	SPAN1
Wall	96.00	Virtual wall (Thermal screen)	ADJACENT	ROOF1_UP
ROOF1_UP				
Roof	23.34	PO film	EXTERNAL	W_90_25
Roof	23.34	PO film	EXTERNAL	W_90_50
Roof	23.34	PO film	EXTERNAL	H_0_0
Roof	23.34	PO film	EXTERNAL	E_270_50
Roof	23.34	PO film	EXTERNAL	E_270_25
Wall	4.45	PO film	ADJACENT	OUTZONE_BACK
Wall	4.45	PO film	ADJACENT	OUTZONE_FRONT2
Wall	7.20	PO film	ADJACENT	SIDE1
Wall	7.20	Virtual wall	ADJACENT	ROOF2_UP
Wall	96.00	Virtual wall (Thermal screen)	ADJACENT	ROOF1_DOWN

.
.
.

SPAN8				
Wall	15.20	PO film	ADJACENT	OUTZONE_BACK
Wall	15.20	PO film	ADJACENT	OUTZONE_FRONT1
Wall	91.20	PO film	ADJACENT	SIDE2
Wall	96.00	Virtual wall	ADJACENT	ROOF8_DOWN
Wall	91.20	Virtual wall (Thermal screen)	ADJACENT	SPAN7
Floor	96.00	Gravel	BOUNDARY	
ROOF1_DOWN				
Wall	1.60	PO film	ADJACENT	OUTZONE_BACK
Wall	1.60	PO film	ADJACENT	OUTZONE_FRONT1
Wall	9.60	PO film	ADJACENT	SIDE2
Wall	9.60	Virtual wall	ADJACENT	ROOF7_DOWN
Wall	96.00	Virtual wall (Thermal screen)	ADJACENT	SPAN8
Wall	96.00	Virtual wall (Thermal screen)	ADJACENT	ROOF8_UP
ROOF1_UP				
Roof	23.34	PO film	EXTERNAL	W_90_25
Roof	23.34	PO film	EXTERNAL	W_90_50
Roof	23.34	PO film	EXTERNAL	H_0_0

Roof	23.34	PO film	EXTERNAL	E_270_50
Roof	23.34	PO film	EXTERNAL	E_270_25
Wall	4.45	PO film	ADJACENT	OUTZONE_BACK
Wall	4.45	PO film	ADJACENT	OUTZONE_FRONT2
Wall	7.20	PO film	ADJACENT	SIDE2
Wall	7.20	Virtual wall	ADJACENT	ROOF7_UP
Wall	96.00	Virtual wall (Thermal screen)	ADJACENT	ROOF8_DOWN

Multi-zone components in the designed greenhouse were used to simulate the energy exchange at the cladding in TRNSYS simulation studio (Fig. 23). In this module, weather data were used as input data and the solar radiation on each wall, the dew-point temperature, and the sky temperature were calculated at each component and transferred to the greenhouse component to simulate the energy exchange by conduction and radiation.

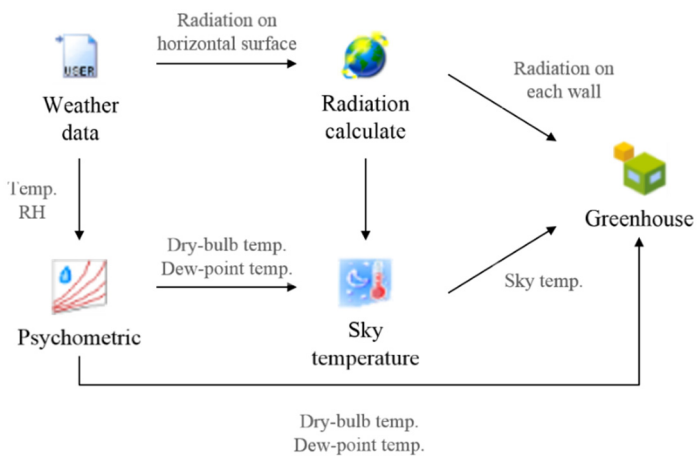

Fig. 23 BES modules for the energy exchange in the cladding of the greenhouse

A switch component was used to design the thermal screen, heat pump and ventilator in the greenhouse (Fig. 24). The internal ambient temperature, amount of external solar radiation, and ambient temperature were used as input data to generate the operating signal of each equipment. The operating signal can take a value of 0 or 1, and when this value is 1, the equipment operates. The operating conditions of each

equipment are determined by Eq. 20, Eq. 21, and Eq. 22, and the operating temperature is established based on the optimum temperature of Irwin mango plants according to the growth period (Table 2).

$$TSSIGN = \begin{cases} 1 & (R_G = 0) \\ 0 & (R_G > 0) \end{cases} \quad \text{Eq. 20}$$

$$HEATSIGN = \begin{cases} 1 & (T_{in} < HEATTEMP) \\ 0 & (T_{in} \geq HEATTEMP) \end{cases}$$
$$COOLSIGN = \begin{cases} 1 & (T_{in} > COOLTEMP) \\ 0 & (T_{in} \leq COOLTEMP) \end{cases} \quad \text{Eq. 21}$$

$$VENTSIGN = \begin{cases} 1 & (T_{in} > VENTTEMP \ \ and \ \ T_{in} > T_{out}) \\ 0 & (T_{in} \leq VENTTEMP) \end{cases} \quad \text{Eq. 22}$$

Where, $TSSIGN$ is a thermal screen signal, $HEATSIGN$ is a heating signal, $HEATTEMP$ is a set temperature of heating, $COOLSIGN$ is a cooling signal, $COOLTEMP$ is a set temperature of cooling, $VENTSIGN$ is a ventilation signal, $VENTTEMP$ is a set temperature of ventilation, T_{in} is an internal ambient temperature (℃), and T_{out} is an external ambient temperature (℃).

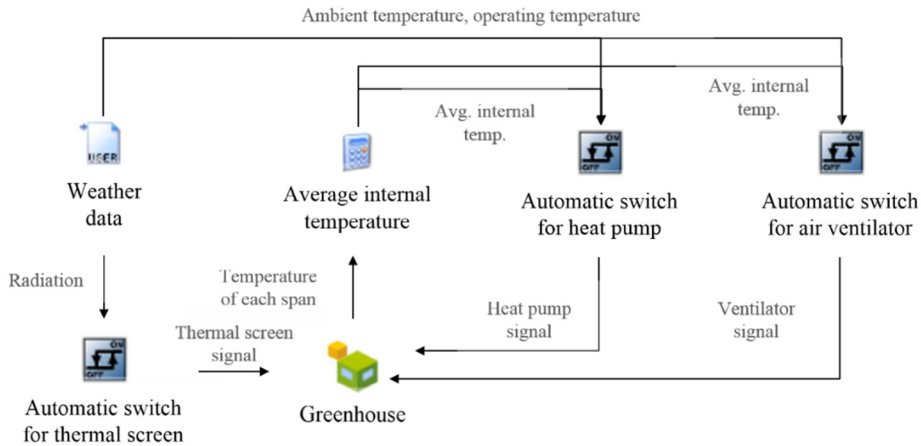

Fig. 24 BES modules for generating the operational signal of the thermal screen, heat pump, air ventilator in the greenhouse

4.2.2. Crop energy exchange modeling

Eq. 5 and Eq. 9 were modified to simulate the energy exchange by the crops. The temperature factor according to Eq. 5 and the humidity factor from Eq. 9 were multiplied by the measured average LAI of the cultivated crops (Eq. 23 and Eq. 24).

$$H = \frac{LAI\rho_a c_p}{r_e}(T_L - T_a) \qquad \text{Eq. 23}$$

$$LE = \frac{\delta}{\delta + \gamma^*}(R_G - G) + \frac{\delta}{\delta + \gamma^*} LAI\rho_a \lambda (e_a^* - e_a) \div r_e \qquad \text{Eq. 24}$$

$$\left(\gamma^* = \gamma\left(1 + \frac{r_s}{r_e}\right)\right)$$

The external resistance of the Irwin mango plants was determined in real time based on Eq. 10. The characteristic leaf dimension was measured for three crops to represent each growth stage of Irwin mango in the greenhouse, and the average value was calculated and found to be 9.99 cm. As the average measured air velocity in the greenhouse was lower than 0.1 m/s, the wind speed for Eq. 10 was set to 0.1 m/s, identical to the value used by Stanghellini. Eq. 18 was used to determine the stomatal resistance, and the measured average LAI of cultivated crops of 1.78 was used as a constant on the assumption that crops are pruned during the experimental period. The real time environmental conditions of a field experiment were used to simulate the plant energy exchange model. These results are shown in Fig. 25.

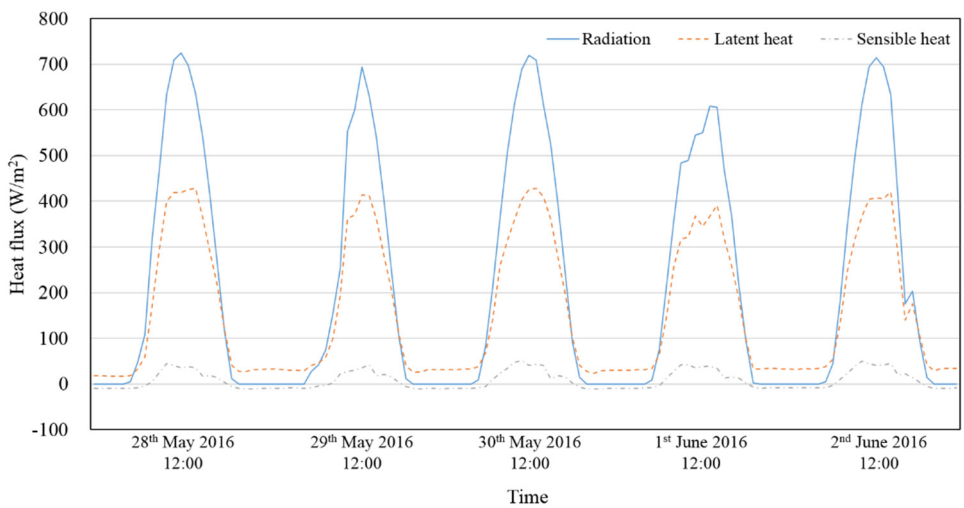

Fig. 25 The latent and sensible heat flux of crops according to time (28th May 2016 ~ 1st June 2016)

Positive values indicate energy flow from the ambient air to the plants, and negative values indicate the opposite case. As solar radiation increased in the daytime, energy exchange by the plants also increased, with energy entirely flowing from the air to the plants. Whereas in the nighttime, energy exchange by the plants dropped dramatically due to the decreased amount of radiation, with the energy flow mainly

due to the vapor pressure deficit between the plants and the surrounding air. Moreover, the surface temperatures of the leaf are higher than the ambient temperature; therefore, sensible heat flux forms from the plants to the air. The BES modules for the plant energy exchange are shown in Fig. 26.

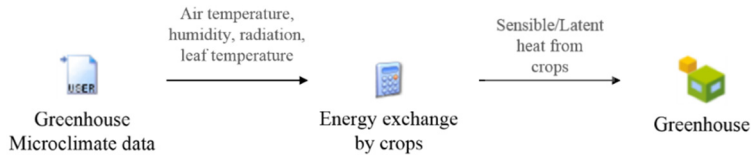

Fig. 26 BES modules for plant energy exchange

The ratio of the sensible and latent heat of crops to external radiation was used to calculate the energy loads. Each proportion were calculated based on five-day simulated data. In the daytime, plants are modeled to absorb thermal energy at proportions of 67.0% by latent heat and 5.3% by sensible heat of the external radiation. At nighttime, plants are modeled to absorb thermal energy of 29.54 W/m^2 by latent heat and to emit thermal energy of 9.49 W/m^2 by sensible heat.

4.2.3. Thermal effluent – heat pump modeling

The performance data of the heat pump in the target greenhouse was modified based on a test report from the target heat pump. The rated air flow and water flow were set to 2,405 and 2.11 l/s, respectively, and the cooling capacity, heating capacity, and power consumption were set for several inlet water temperatures. For cooling, parts of the thermal energy in the greenhouse were removed by latent heat due to vapor condensation, whereas for heating, all energy was transferred by sensible heat. The cooling performance data for inlet water temperatures of 1, 5, and 10 ℃ were extrapolated based on data for inlet water temperatures of 15, 20, 25, and 30 ℃

(Table 9). The heating performance data for inlet water temperatures of 1 and 30 ℃ were also extrapolated based on data for inlet water temperatures of 5, 10, 15, 20, and 25 ℃ (Table 10).

Table 9 Cooling performance data of heat pump in the target greenhouse

Water temperature (℃)	Total cooling capacity (kW)	Sensible cooling capacity (kW)	Power consumption (kW)
1	41.38	33.93	4.92
5	39.00	31.98	5.92
10	37.10	30.42	6.72
15	35.20	28.86	7.52
20	33.30	27.31	8.32
25	31.30	25.67	9.24
30	29.30	24.03	10.30

Table 10 Heating performance data of heat pump in the target greenhouse

Water temperature (℃)	Total heating capacity (kW)	Power consumption (kW)
1	30.08	8.42
5	37.77	8.47
10	43.92	8.52
15	51.00	8.60
20	59.01	8.71
25	68.15	8.85
30	77.29	8.99

The performance correction data were established to consider changes in the performance and the power consumption of heat pump due to the changes of the greenhouse internal air temperature and humidity. Each multiplier was configured for dry bulb temperatures of 5, 10, 15, 20, 25, 30, and 35 ℃, and wet bulb temperatures of 1, 5, 10, 15, 20, 25, and 30 ℃ (Table 11 and Table 12).

Table 11 Cooling performance correction data of heat pump in the target greenhouse

Dry bulb temperature (℃)	Wet bulb temperature (℃)	Multipliers of total cooling capacity	Multipliers of sensible cooling capacity	Multipliers of power consumption
5	1	0.85	1.00	0.94
10	1	0.85	1.18	0.94
10	5	0.90	1.00	0.96
15	1	0.85	1.36	0.94
15	5	0.90	1.18	0.96
15	10	0.95	1.00	0.98
20	1	0.85	1.54	0.94
20	5	0.90	1.36	0.96
20	10	0.95	1.18	0.98
20	15	1.00	1.00	1.00
25	1	0.85	1.30	0.94
25	5	0.90	1.54	0.96
25	10	0.95	1.36	0.98
25	15	1.00	1.18	1.00
25	20	1.05	1.00	1.02
30	1	0.85	1.15	0.94
30	5	0.90	1.30	0.96
30	10	0.95	1.54	0.98
30	15	1.00	1.36	1.00
30	20	1.05	1.18	1.02
30	25	1.10	1.00	1.04
35	1	0.85	1.13	0.94
35	5	0.90	1.15	0.96
35	10	0.95	1.30	0.98
35	15	1.00	1.54	1.00
35	20	1.05	1.36	1.02
35	25	1.10	1.18	1.04
35	30	1.15	1.00	1.06

Table 12 Heating performance correction data of heat pump in the target greenhouse

Dry bulb temperature (℃)	Multipliers of total cooling capacity	Multipliers of power consumption
5	1.06	0.76
10	1.04	0.84
15	1.02	0.92
20	1.00	1.00
25	0.98	1.08
30	0.96	1.16
35	0.94	1.24

Real time thermal effluent data was used to calculate the rated cooling and heating capacities and the power consumption. The greenhouse internal air temperature and humidity level were considered simultaneously to calculate the actual energy production and power consumption levels. The actual calculated energy production and power consumption levels were compared with the energy loads of the target greenhouse to simulate the energy consumption of the target greenhouse. The BES modules for the thermal effluent – heat pump system are shown in Fig. 27.

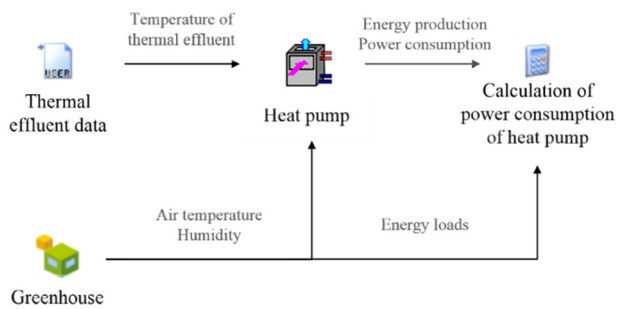

Fig. 27 BES modules for the thermal effluent – heat pump system

The dynamic energy exchange model of greenhouse was designed based on BES technique including the greenhouse structure, crop energy exchange model, and thermal effluent – heat pump system (Fig. 28). Each parts are connected to greenhouse to simulate simultaneously.

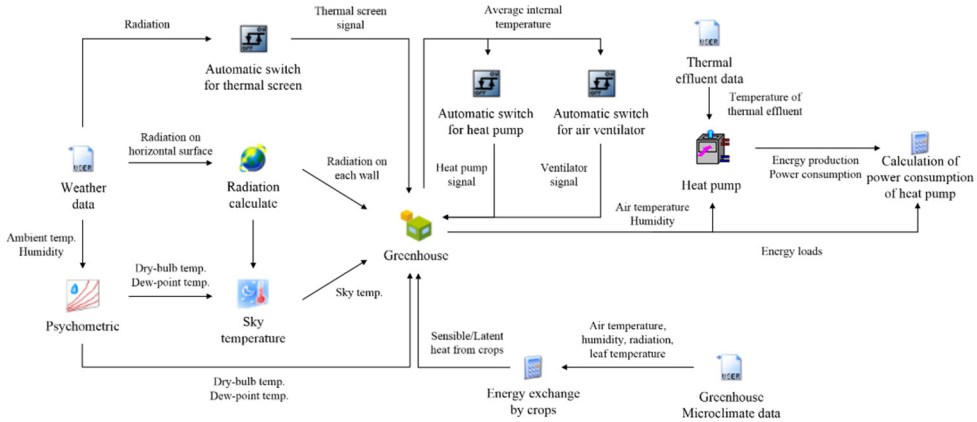

Fig. 28 BES model for calculating the energy loads of the greenhouse

4.3. Validation of the greenhouse BES model

4.3.1. Validation of transpiration by crops

In order to validate the plant energy exchange model, the transpiration rate measured by the field experiment was used in a comparison with the simulated data. Measured data at five-minute intervals and simulated data at one-minute intervals as calculated based on Eq. 16 and Eq. 24, respectively, were averaged over a period of one hour and compared (Fig. 29). The designed plant energy exchange model was verified to be able to provide a good estimation of the change of the transpiration rate throughout the experimental period ($R^2 = 0.96$, $d = 0.99$). In the daytime of the 28^{th} of May of 2016, the measured data were shown to be somewhat lower than the simulated data, as half of one liter of water was added by irrigation at 9:00 AM in every case, usually, while during the experimental period, a liter of water was added in this manner in every case at 9:00 PM. As the equation used in this study is a modified version of the Penman-Monteith equation, the plants transpire on the assumption that they are well irrigated. This assumption is considered in the simulation, whereas the actual plants were not fully irrigated during the daytime on the 28^{th} of May of 2016 which was a source of error. Considering this error factor, with a dataset of four days set except for the first date, the plant energy exchange model designed in this study was found to be able to reflect the actual latent heat from the plants well.

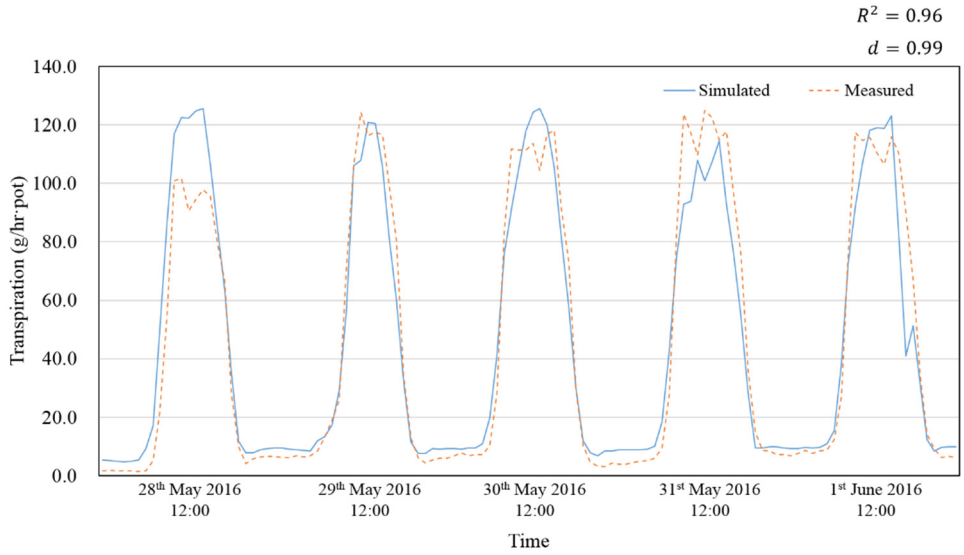

Fig. 29 Validation results of the plant energy exchange module by comparing the transpiration rate (28^{th} May 2016 to 1^{st} June 2016)

4.3.2. Validation of the greenhouse internal temperature

In order to validate the greenhouse dynamic energy exchange model, the measured greenhouse internal air temperature was compared with the simulated data. The hourly internal air temperatures were calculated based on five-second intervals measured data from 15 locations and one-minute intervals simulated data and compared (Fig. 30). The average value of the internal air temperature at 15 locations is indicated by the dot in the figure, and the standard deviation is displayed as error bars. The simulated data is the average air temperature of the plant growth room overall.

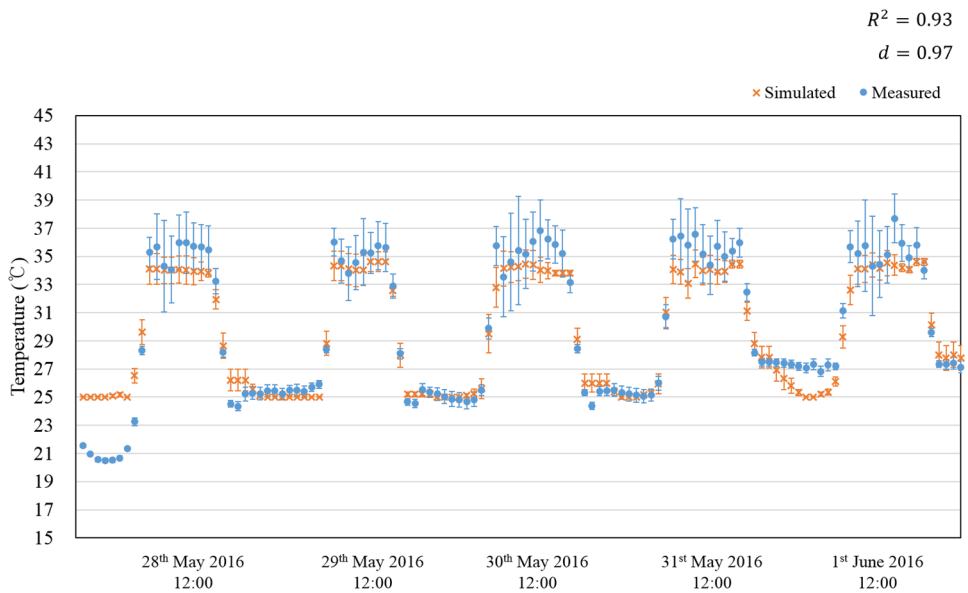

Fig. 30 Validation results for the greenhouse energy exchange model in a comparison with the internal air temperature of the greenhouse (28th May 2016 to 1st June 2016)

In the daytime, the internal air temperature increased due to an increase in solar radiation, while in the nighttime, the heat pump operated based on a set temperature to maintain the internal air temperature. The simulated data typically follow the measured data; however, on the nights of the 27th and 31st of May, the internal air temperature differed considerably from those on other days. According to the data logger, on the night of the 27th, the heat pump did not operate while on the night of the 31st, the set temperature of the heat pump changed from 25 ℃ to 27 ℃. Therefore, the working schedule of the heat pump was modified and the designed greenhouse dynamic energy exchange model was verified to be able to provide a good estimation of the change of the internal air temperature throughout the experimental period (R^2 = 0.97, d = 0.99) (Fig. 31).

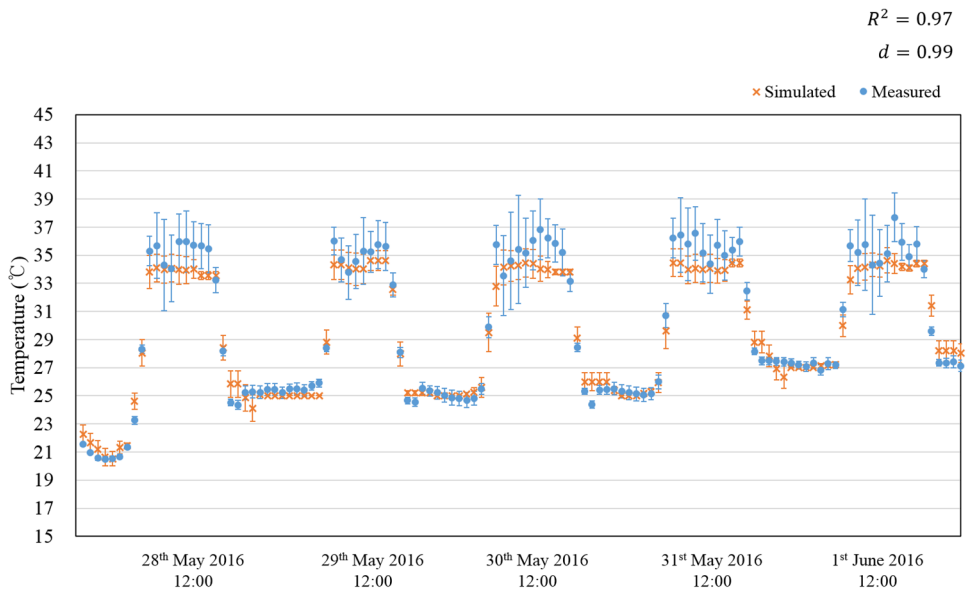

Fig. 31 Modified validation results for greenhouse energy exchange model through a comparison of the internal air temperature of the greenhouse (28th May 2016 to 1st June 2016)

4.4. Calculation of the energy load according to the growth stage

4.4.1. Periodic energy loads

The periodic energy loads over a course of nine years were calculated. Table 13 shows the calculation result of the periodic energy loads during the vegetation and floral-initiation periods. Calculated cooling loads were relatively high as compared to the heating loads throughout both periods. As the vegetation period and floral-initiation period of Irwin mango start in summer, heating loads seldom occurred for the two periods. Moreover, the set temperature of the heat pump for cooling was changed from 30 ℃ to 20 ℃ as the growth period progressed; therefore, the average periodic cooling loads increased from 110,750 MJ to 186,037 MJ, representing an increase of approximately 68%.

Table 13 Periodic energy loads for the vegetation and floral-initiation period (Unit: MJ)

Year	Vegetation		Floral-initiation	
	Cooling loads	Heating loads	Cooling loads	Heating loads
2006 ~ 2007	102,642	900	206,664	0
2007 ~ 2008	94,137	134	182,316	0
2008 ~ 2009	114,304	722	193,954	0
2009 ~ 2010	115,108	709	200,422	0
2010 ~ 2011	128,023	334	194,651	0
2011 ~ 2012	84,638	886	177,179	78
2012 ~ 2013	140,485	50	157,282	0
2013 ~ 2014	114,069	203	198,964	3
2014 ~ 2015	103,348	65	162,904	0
Average	110,750	445	186,037	9

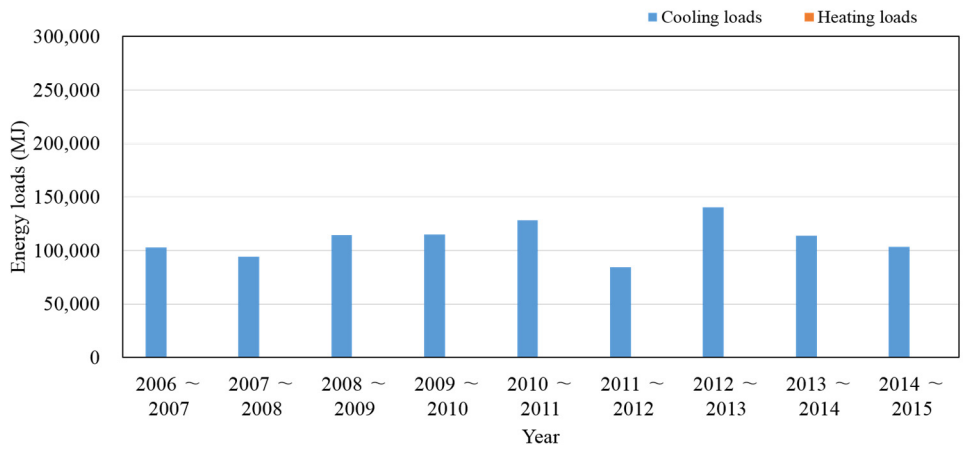

Fig. 32 Periodic energy loads of the vegetation period by year

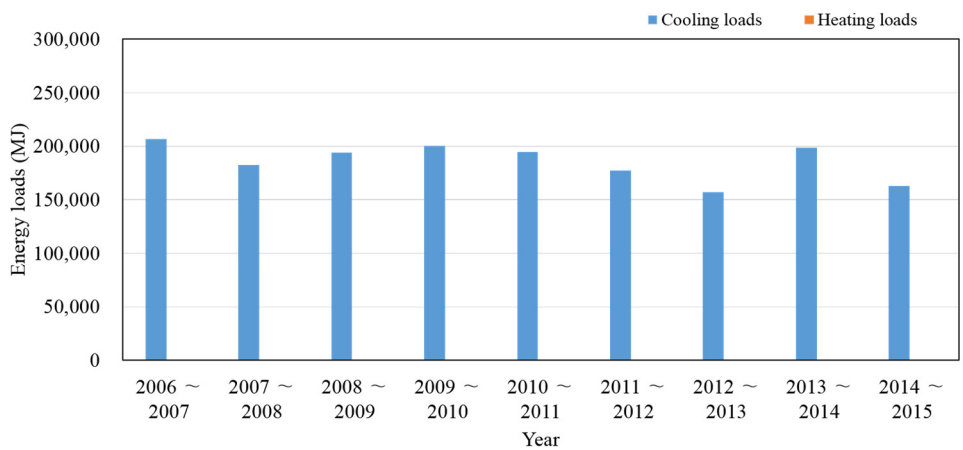

Fig. 33 Periodic energy loads of the floral-initiation period by year

The cooling and heating loads vary depending on the year, as shown in Fig. 32 and Fig. 33. The variation for the different years can be explained in terms of the average external air temperature and solar radiation (Table 14). The cooling loads are mainly caused by increases in the external air temperature and solar radiation, causing the internal air temperature to rise. Therefore, as the average external air temperature and solar radiation was high, the periodic cooling loads were also increased. For example, in the years of 2012 ~ 2013, when the average air

temperature was 24.4 ℃ and the average solar radiation was 722 kJ/hr, somewhat higher than those of the other years, the periodic cooling load was 140,485 MJ which was 26.8% higher than the average periodic cooling load. In comparison to the years of 2009 ～ 2010 years, when the average solar radiation was similar to the years of 2012 ～ 2013, the periodic cooling load was 18.1% lower because the average air temperature was 1.6 ℃ lower. For a similar reason, in the years of 2013 ～ 2014, the periodic cooling load was 18.8% lower than the years of 2012 ～ 2013 because the average solar radiation was 99.6 kJ/hr lower.

Table 14 Weather condition of the vegetation and floral-initiation period

Year	Vegetation		Floral-initiation	
	Average air temperature (℃)	Average solar radiation (kJ/hr)	Average air temperature (℃)	Average solar radiation (kJ/hr)
2006 ～ 2007	22.9	655	21.2	628
2007 ～ 2008	23.3	622	21.0	545
2008 ～ 2009	23.6	677	20.6	621
2009 ～ 2010	22.8	736	20.3	666
2010 ～ 2011	23.9	730	21.3	565
2011 ～ 2012	23.1	577	19.5	610
2012 ～ 2013	24.4	722	20.1	491
2013 ～ 2014	24.5	623	21.1	586
2014 ～ 2015	23.4	640	20.1	521

Table 15 shows the calculated results of the periodic energy loads during the flowering and fruit-bearing periods. As the season changes from summer to autumn, the cooling loads decrease and the heating loads increase compared to the energy loads during the vegetation and floral-initiation periods. In the flowering period, the heating loads were higher than the cooling loads while in the fruit-bearing period, no cooling loads were noted. The set temperature of the heat pump for cooling changed from 25 ℃ to 30 ℃; therefore, the average periodic cooling loads changed from 5,665 MJ to 0 MJ. For the periodic heating loads, the set temperature of the heat

pump for heating was changed from 18 ℃ to 22 ℃; hence, the average periodic heating loads increased from 196,943 MJ to 253,089 MJ, i.e., approximately 29%.

Table 15 Periodic energy loads of the flowering and fruit-bearing periods (Unit: MJ)

Year	Flowering		Fruit-bearing	
	Cooling loads	Heating loads	Cooling loads	Heating loads
2006 ~ 2007	8,017	172,453	0	222,575
2007 ~ 2008	5,314	191,398	0	260,988
2008 ~ 2009	4,002	179,728	0	231,479
2009 ~ 2010	8,164	194,840	0	261,835
2010 ~ 2011	5,392	195,376	0	278,135
2011 ~ 2012	7,790	175,620	0	265,026
2012 ~ 2013	3,427	238,982	0	273,586
2013 ~ 2014	5,412	209,481	0	240,603
2014 ~ 2015	3,470	214,613	0	243,576
Average	5,665	196,943	0	253,089

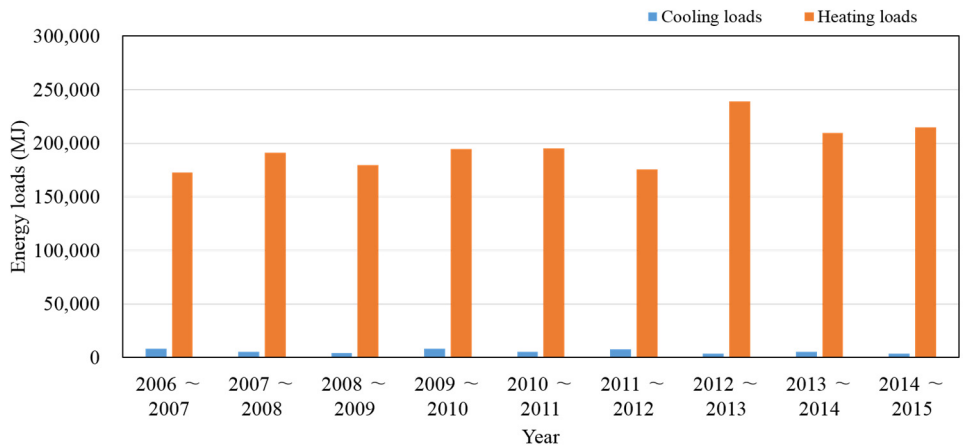

Fig. 34 Periodic energy loads of the flowering period by year

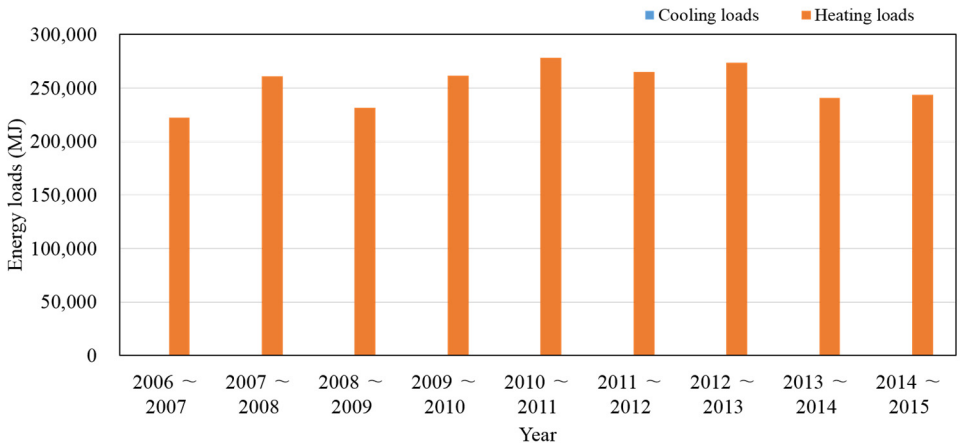

Fig. 35 Periodic energy loads of the fruit-bearing period by year

The cooling and heating loads vary depending on the year, as in the previous growth periods (Fig. 34 and Fig. 35). The coefficients of variation of the heating loads which mainly occurred during these periods were calculated and found to be 0.108 during the flowering period and 0.076 during the fruit-bearing period. This can be explained in terms of the average external air temperature and solar radiation (Table 16). The heating loads are mainly caused by decreases in the external air temperature and solar radiation level, causing the internal air temperature to decrease. During 2012 ~ 2013, when the periodic heating loads of the flowering period were higher than those of any other year, the average air temperature was 4.0 ℃ and the average solar radiation was 314 kJ/hr, lower than in the other years. Whereas in 2006 ~ 2007, when the periodic heating loads of the flowering period were lower than in any other year, the average air temperature was 7.2 ℃ and the average solar radiation was 354 kJ/hr, higher than in the other years. For the same reason, during the periods of 2008 ~ 2009 and 2011 ~ 2012, when the periodic heating loads of the flowering period were relatively high, the average external air temperature and solar radiation were higher than they were in 2013 ~ 2014 and 2014 ~ 2015, when the periodic heating loads were relatively low. During the fruit-bearing period,

the periodic heating loads were also varied by the average external air temperature and solar radiation level. Additionally, the average external air temperature for the entire year changed from 5.7 ℃ to -3.5 ℃ as the growth period progressed, which may also be the reason behind the increase in the periodic heating loads.

Table 16 Weather condition of the flowering and fruit-bearing period

Year	Flowering		Fruit-bearing	
	Average air temperature (℃)	Average solar radiation (kJ/hr)	Average air temperature (℃)	Average solar radiation (kJ/hr)
2006 ~ 2007	7.2	354	-0.4	372
2007 ~ 2008	6.1	353	1.3	365
2008 ~ 2009	6.9	329	-1.9	399
2009 ~ 2010	6.5	326	0.9	350
2010 ~ 2011	5.6	390	-1.3	340
2011 ~ 2012	7.3	343	-3.6	424
2012 ~ 2013	4.0	314	-2.2	394
2013 ~ 2014	5.5	326	-2.1	326
2014 ~ 2015	5.5	286	0.3	327

Table 17 shows the calculated results of the periodic energy loads during the fruit-growing and harvesting periods. In the fruit-growing period, the internal air temperature of the greenhouse should be maintaining at more than 25 ℃ in the winter season; therefore, heating loads were noted to have occurred more relative to cooling loads, whereas the periodic cooling and heating loads were similar during the harvesting period because the internal air temperature of the greenhouse was maintained in the range of 25 ~ 30 ℃. As growth period progressed, the average periodic cooling loads increased from 235,938 MJ to 67,927 MJ, representing an increase of approximately 71%.

Table 17 Periodic energy loads of the fruit-growing and harvesting periods (Unit: MJ)

Year	Fruit-growing		Harvesting	
	Cooling loads	Heating loads	Cooling loads	Heating loads
2006 ~ 2007	3,006	222,404	36,076	66,521
2007 ~ 2008	6,456	234,507	37,831	61,399
2008 ~ 2009	8,417	224,465	43,611	70,166
2009 ~ 2010	2,482	242,439	28,214	78,921
2010 ~ 2011	3,868	238,209	30,119	72,790
2011 ~ 2012	1,734	263,188	48,892	56,545
2012 ~ 2013	2,611	247,898	31,766	83,232
2013 ~ 2014	5,690	215,901	42,189	58,218
2014 ~ 2015	2,706	234,429	38,318	63,553
Average	4,108	235,938	37,446	67,927

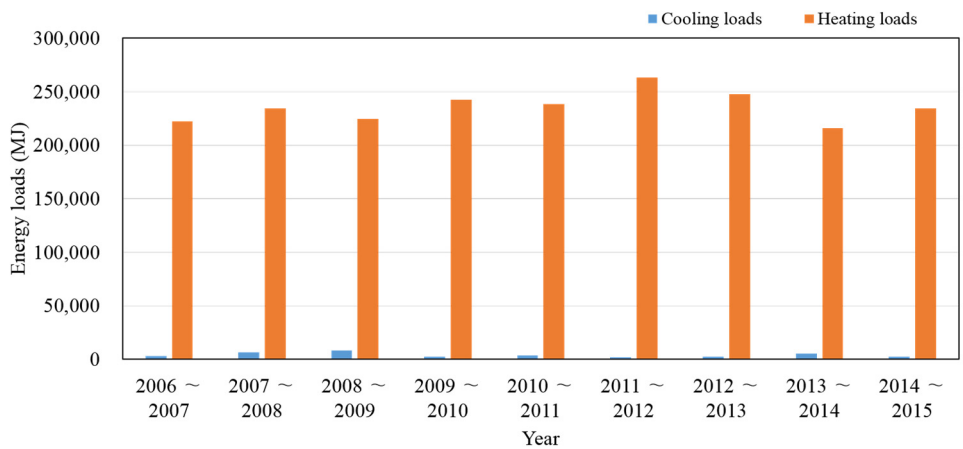

Fig. 36 Periodic energy loads of the fruit-growing period by year

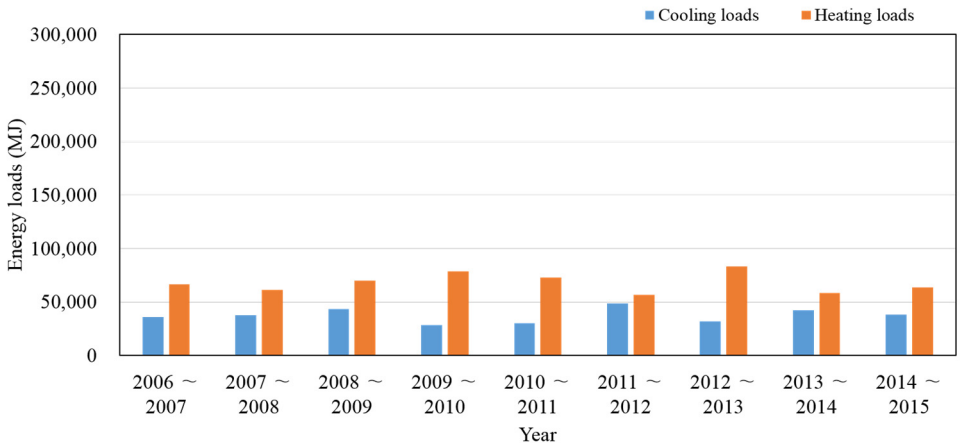

Fig. 37 Periodic energy loads of the harvesting period by year

The changes in the periodic cooling and heating loads by year are shown in Fig. 36 and Fig. 37, respectively. The relation between weather condition and the cooling and heating loads can be figured out through Table 18. In the fruit-growing period, as the average air temperature and solar radiation for a specific year were low, the periodic heating loads were higher than those of the other years. On the other hand, during the harvesting period, there is a negative correlation between the periodic heating loads and the periodic cooling loads based on the changes of the average air temperature and solar radiation. The set temperature of the heat pump for heating during the two periods was identical; however, the average periodic heating loads both decreased because the average air temperature and solar radiation level increased. The average air temperature and solar radiation level during the harvesting period were correspondingly 14.8 ℃ and 769 kJ/hr, higher than those during the fruit-growing period by 9.6 ℃ and 168 kJ/hr, respectively.

Table 18 Weather condition of the fruit-growing and harvesting period

Year	Fruit-growing		Harvesting	
	Average air temperature (℃)	Average solar radiation (kJ/hr)	Average air temperature (℃)	Average solar radiation (kJ/hr)
2006 ~ 2007	5.0	606	14.2	755
2007 ~ 2008	6.1	578	14.9	783
2008 ~ 2009	5.4	629	15.2	788
2009 ~ 2010	5.8	630	15.1	802
2010 ~ 2011	5.4	540	13.8	739
2011 ~ 2012	4.3	672	14.6	729
2012 ~ 2013	3.9	579	16.1	836
2013 ~ 2014	4.2	606	14.0	705
2014 ~ 2015	6.6	571	15.8	785

4.4.2. Maximum energy loads

The maximum energy loads over a period of nine years were calculated based on the optimum growth temperature of Irwin mango plants. Table 19 shows the maximum cooling and heating loads during the vegetation period and the time of their occurrence for each year. The average maximum cooling and heating loads were calculated and found to be 361,875 and 16,475 kJ/hr, respectively. The maximum cooling loads usually occurred at around 1:00 PM to 2:00 PM, when the external air temperature and solar radiation were highest during the day, whereas, the maximum heating loads usually occurred at around 3:00 AM to 5:00 AM, when the external air temperature and the solar radiation level reached their lowest points of the day.

Table 19 Maximum energy loads of the vegetation period

Year	Maximum cooling loads		Maximum heating loads	
	Loads (kJ/hr)	Occurrence	Loads (kJ/hr)	Occurrence
2006 ~ 2007	396,231	Aug. 08, 2006 13:00	56,850	Apr. 11, 2006 03:00
2007 ~ 2008	382,420	Aug. 11, 2007 13:00	29,923	June 02, 2007 04:00
2008 ~ 2009	409,592	Aug. 10, 2008 13:00	64,093	June 06, 2008 04:00
2009 ~ 2010	387,674	Aug. 09, 2009 13:00	54,327	June 04, 2009 04:00
2010 ~ 2011	386,916	Aug. 05, 2010 13:00	55,001	June 01, 2010 04:00
2011 ~ 2012	408,142	July 19, 2011 13:00	51,450	June 02, 2011 04:00
2012 ~ 2013	429,874	Aug. 05, 2012 13:00	11,134	June 03, 2012 04:00
2013 ~ 2014	360,402	Aug. 01, 2013 13:00	37,901	June 02, 2013 04:00
2014 ~ 2015	361,875	July 30, 2014 14:00	16,475	June 03, 2014 05:00
Average	391,458	-	41,906	-

Table 20 is the external air temperature and solar radiation level on the corresponding time when the maximum cooling and heating loads occurred on the vegetation period. As the maximum cooling load usually occurred in the middle of the day, the maximum cooling loads are negatively correlated with external air temperature and the level of solar radiation. During the periods of 2008 ~ 2009 and 2012 ~ 2013, when the external air temperature was relatively high, the maximum corresponding cooling loads were 409,592 and 429,874 kJ/hr, 4.6 and 9.8% higher than the average maximum cooling load, respectively. In contrast, for the periods of 2013 ~ 2014 and 2014 ~ 2015, when the external air temperature was relatively low, the maximum corresponding cooling loads were 360,402 and 361,875 kJ/hr, i.e., 7.9 and 7.6% lower than the average maximum cooling load, respectively. If the external air temperature is similar, the maximum cooling load is positively correlated with the level of solar radiation. The maximum heating load typically occurred at dawn, and it is negatively correlated with the external air temperature.

Table 20 Weather condition of the vegetation period when maximum energy loads occurred

Year	Maximum cooling loads		Maximum heating loads	
	Air temperature (℃)	Solar radiation (kJ/hr)	Air temperature (℃)	Solar radiation (kJ/hr)
2006 ~ 2007	5.0	606	14.2	755
2007 ~ 2008	6.1	578	14.9	783
2008 ~ 2009	5.4	629	15.2	788
2009 ~ 2010	5.8	630	15.1	802
2010 ~ 2011	5.4	540	13.8	739
2011 ~ 2012	4.3	672	14.6	729
2012 ~ 2013	3.9	579	16.1	836
2013 ~ 2014	4.2	606	14.0	705
2014 ~ 2015	6.6	571	15.8	785

Table 21 shows the maximum cooling and heating loads during the floral-initiation period and the corresponding time of occurrence for each year. The

maximum cooling loads mainly occurred at around 12:00 PM to 1:00 PM, whereas the maximum heating loads occurred at around 5:00 PM. In the floral-initiation period, as the internal air temperature of the greenhouse should be maintained in the range of 8 ~ 20 ℃ in the summer season, a cooling load mainly occurred rather than a heating load. The average maximum cooling load was 498,413 kJ/hr, and the maximum heating load did not occur except for the periods of 2011 ~ 2012 and 2013 ~ 2014.

Table 21 Maximum energy loads of the floral-initiation period

Year	Maximum cooling loads		Maximum heating loads	
	Loads (kJ/hr)	Occurrence	Loads (kJ/hr)	Occurrence
2006 ~ 2007	511,516	Aug. 15, 2006 12:00	-	-
2007 ~ 2008	512,707	Aug. 24, 2007 13:00	-	-
2008 ~ 2009	468,915	Aug. 30, 2008 13:00	-	-
2009 ~ 2010	527,512	Aug. 15, 2009 13:00	-	-
2010 ~ 2011	518,703	Aug. 19, 2010 13:00	-	-
2011 ~ 2012	485,559	Aug. 31, 2011 13:00	29,426	Oct. 18, 2011 05:00
2012 ~ 2013	495,327	Aug. 26, 2012 13:00	-	-
2013 ~ 2014	507,755	Aug. 21, 2013 13:00	3,215	Oct. 17, 2013 05:00
2014 ~ 2015	457,721	Sep. 06, 2014 13:00	-	-
Average	498,413	-	-	-

Table 22 is the external air temperature and solar radiation level on the corresponding time when the maximum cooling and heating loads occurred on the floral-initiation period. In 2012 ~ 2013, when the external air temperature was highest during the analysis period, the maximum cooling load was 495,327 kJ/hr, similar to the average value due to the relatively low solar radiation. On the other

hand, for the periods of 2009 ~ 2010 and 2010 ~ 2011, when the external air temperature and solar radiation level were both relatively high, the maximum cooling loads were 527,512 and 518,703 kJ/hr, 5.8 and 4.1% higher than the average maximum cooling load, respectively. However, for 2006 ~ 2007, when the external air temperature and solar radiation level were higher than those of 2009 ~ 2010, the maximum cooling load was lower than that that for 2009 ~ 2010. This result may be due to the fact that BES considers the thermal storage of the cladding, plants, soils and other factors.

Table 22 Weather condition of the floral-initiation period when maximum energy loads occurred

Year	Maximum cooling loads		Maximum heating loads	
	Air temperature (℃)	Solar radiation (kJ/hr)	Air temperature (℃)	Solar radiation (kJ/hr)
2006 ~ 2007	31.3	3,280	-	-
2007 ~ 2008	30.9	2,910	-	-
2008 ~ 2009	29.1	2,990	-	-
2009 ~ 2010	31.4	2,990	-	-
2010 ~ 2011	30.9	3,120	-	-
2011 ~ 2012	30.5	2,770	2.9	0
2012 ~ 2013	32.0	2,590	-	-
2013 ~ 2014	31.3	2,700	6.3	0
2014 ~ 2015	29.6	2,700	-	-

Table 23 shows the maximum cooling and heating loads during the flowering period and the time of occurrence for each year. As the flowering period of Irwin mango starts in the autumn and ends in the winter season, the maximum cooling load and heating load occurred relatively evenly as compared to the other growth periods. The maximum cooling load usually occurred at around 1:00 PM to 2:00 PM in the autumn and the maximum heating load usually occurred at around 3:00 AM to 7:00 AM in the winter season. The average maximum cooling and heating loads were 175,649 and 338,727 kJ/hr, respectively.

Table 23 Maximum energy loads of the flowering period

Year	Maximum cooling loads		Maximum heating loads	
	Loads (kJ/hr)	Occurrence	Loads (kJ/hr)	Occurrence
2006 ~ 2007	191,913	Oct. 21, 2006 13:00	340,642	Dec. 30, 2006 05:00
2007 ~ 2008	169,341	Oct. 27, 2007 14:00	303,441	Nov. 19, 2007 06:00
2008 ~ 2009	192,516	Oct. 20, 2008 13:00	346,761	Dec. 06, 2008 03:00
2009 ~ 2010	175,616	Oct. 30, 2009 13:00	347,996	Dec. 27, 2009 06:00
2010 ~ 2011	195,353	Oct. 22, 2010 13:00	348,938	Dec. 25, 2010 05:00
2011 ~ 2012	182,140	Nov. 03, 2011 13:00	339,968	Dec. 27, 2011 03:00
2012 ~ 2013	160,184	Oct. 26, 2012 13:00	384,618	Dec. 26, 2012 05:00
2013 ~ 2014	181,428	Oct. 23, 2013 13:00	309,554	Dec. 13, 2013 07:00
2014 ~ 2015	132,351	Oct. 25, 2014 13:00	326,626	Dec. 17, 2014 07:00
Average	175,649	-	338,727	-

Table 24 is the external air temperature and solar radiation level on the corresponding time when the maximum cooling and heating loads occurred on the flowering period. In the period of 2010 ~ 2011, when the solar radiation level was highest during the analysis period and the air temperature was relatively high, the cooling load was 195,353 kJ/hr, which is 11.2% higher than the average maximum cooling load. Whereas in 2014 ~ 2015, when the air temperature was lowest during the analysis period, the maximum cooling load was 132,351 kJ/hr, 24.7% lower than the average maximum cooling load. As the maximum heating load mainly occurred at dawn when the solar radiation level was usually 0, it is directly related to the external air temperature. For this reason, during the period of 2012 ~ 2013, when the air temperature was lowest, the maximum heating load was 384,618 kJ/hr, i.e., 13.5% higher than the average maximum heating load, whereas in the period of 2007 ~ 2008, when the air temperature was highest, the maximum heating load

was 303,441 kJ/hr, 10.4% lower than the average maximum heating load.

Table 24 Weather condition of the flowering period when maximum energy loads occurred

Year	Maximum cooling loads		Maximum heating loads	
	Air temperature (℃)	Solar radiation (kJ/hr)	Air temperature (℃)	Solar radiation (kJ/hr)
2006 ~ 2007	22.9	1,990	-7.0	0
2007 ~ 2008	20.5	1,750	-3.3	0
2008 ~ 2009	24.8	1,920	-10.6	0
2009 ~ 2010	23.4	1,830	-7.8	0
2010 ~ 2011	22.5	2,240	-9.2	0
2011 ~ 2012	22.9	1,860	-8.0	0
2012 ~ 2013	21.8	1,960	-12.5	0
2013 ~ 2014	21.8	2,070	-3.9	0
2014 ~ 2015	20.2	1,850	-7.0	0

Table 25 shows the maximum cooling and heating loads during the fruit-bearing period and the time of occurrence for each year. As the fruit-bearing period of Irwin mango is in the winter season, a cooling load was not noted and the average maximum heating load was 422,061 kJ/hr, higher than that in other growth periods. The maximum heat load usually occurred at around 5:00 AM to 7:00 AM in January.

Table 25 Maximum energy loads of the fruit-bearing period

Year	Maximum cooling loads		Maximum heating loads	
	Loads (kJ/hr)	Occurrence	Loads (kJ/hr)	Occurrence
2006 ~ 2007	-	-	395,349	Jan. 14, 2007 05:00
2007 ~ 2008	-	-	427,721	Jan. 17, 2008 05:00
2008 ~ 2009	-	-	437,214	Jan. 15, 2009 06:00
2009 ~ 2010	-	-	436,286	Jan. 14, 2010 07:00
2010 ~ 2011	-	-	436,842	Jan. 31, 2011 05:00
2011 ~ 2012	-	-	432,090	Feb. 02, 2012 06:00
2012 ~ 2013	-	-	443,143	Jan. 04, 2013 06:00
2013 ~ 2014	-	-	400,004	Jan. 10, 2014 07:00
2014 ~ 2015	-	-	389,904	Jan. 03, 2015 07:00
Average	-	-	422,061	-

Table 26 is the external air temperature and solar radiation level on the corresponding time when the maximum cooling and heating loads occurred on the fruit-bearing period. As the maximum heating load is directly related to the external air temperature, during the period of 2012 ~ 2013, when the air temperature was lowest, the maximum heating load was 443,143 kJ/hr, which is 5.0% higher than the average maximum heating load. In contrast, for the periods of 2006 ~ 2007, 2013 ~ 2014, and 2014 ~ 2015, when the air temperature was relatively high, the maximum corresponding heating loads were 395,349, 400,004, and 389,904 kJ/hr, values which are 6.3, 5.2, and 7.6% lower than the average maximum heating loads, respectively.

Table 26 Weather condition of the fruit-bearing period when maximum energy loads occurred

Year	Maximum cooling loads		Maximum heating loads	
	Air temperature (℃)	Solar radiation (kJ/hr)	Air temperature (℃)	Solar radiation (kJ/hr)
2006 ~ 2007	-	-	-7.4	0
2007 ~ 2008	-	-	-10.9	0
2008 ~ 2009	-	-	-11.4	0
2009 ~ 2010	-	-	-10.5	0
2010 ~ 2011	-	-	-12.5	0
2011 ~ 2012	-	-	-10.9	0
2012 ~ 2013	-	-	-13.6	0
2013 ~ 2014	-	-	-6.2	0
2014 ~ 2015	-	-	-7.0	0

Table 27 shows the maximum cooling and heating loads during the fruit-growing period and the time of occurrence for each year. The fruit-growing period of Irwin mango starts in winter and ends in the spring. Therefore, the maximum cooling load occurred at around 1:00 PM to 2:00 PM in the spring season, whereas the maximum heating load mainly occurred at around 5:00 AM to 6:00 AM in the winter season. The average maximum cooling load was 128,986 kJ/hr and the average maximum heating load was 429,474 kJ/hr, higher than in any of the other growth periods.

Table 27 Maximum energy loads of the fruit-growing period

Year	Maximum cooling loads		Maximum heating loads	
	Loads (kJ/hr)	Occurrence	Loads (kJ/hr)	Occurrence
2006 ~ 2007	99,478	Apr. 14, 2007 13:00	399,497	Feb. 16, 2007 06:00
2007 ~ 2008	166,376	Apr 08, 2008 13:00	461,769	Feb. 18, 2008 06:00
2008 ~ 2009	184,676	Apr. 10, 2009 14:00	465,055	Feb. 17, 2009 06:00
2009 ~ 2010	123,456	Apr. 09, 2010 14:00	401,435	Feb. 17, 2010 05:00
2010 ~ 2011	103,761	Apr. 08, 2011 13:00	420,669	Feb. 15, 2011 00:00
2011 ~ 2012	99,933	Apr. 08, 2012 13:00	469,872	Feb. 19, 2012 06:00
2012 ~ 2013	114,191	Apr. 04, 2013 13:00	452,557	Feb. 20, 2013 06:00
2013 ~ 2014	151,965	Mar. 28, 2014 13:00	412,568	Feb. 21, 2014 06:00
2014 ~ 2015	117,033	Apr. 11, 2015 13:00	381,847	Mar. 05, 2015 05:00
Average	128,986	-	429,474	-

Table 28 is the external air temperature and solar radiation level on the corresponding time when the maximum cooling and heating loads occurred on the fruit-growing period. In 2007 ~ 2008, when the external air temperature and solar radiation were relatively high, the maximum cooling load was 184,676 kJ/hr, which is 43.2% higher than the average maximum cooling load, whereas in 2007 ~ 2008, when the external air temperature and solar radiation level were relatively low, the maximum cooling load was 99,478 kJ/hr, which is 22.9% lower than the average maximum cooling load. In the case of the maximum heating load, in 2011 ~ 2012, when the external air temperature was lowest, it was 469,872 kJ/hr, representing a 9.4% increase over the average maximum heating load.

Table 28 Weather condition of the fruit-growing period when maximum energy loads occurred

Year	Maximum cooling loads		Maximum heating loads	
	Air temperature (℃)	Solar radiation (kJ/hr)	Air temperature (℃)	Solar radiation (kJ/hr)
2006 ~ 2007	14.3	2,520	-3.8	0
2007 ~ 2008	20.5	2,960	-7.9	0
2008 ~ 2009	20.9	3,130	-8.2	0
2009 ~ 2010	17.0	2,810	-5.9	0
2010 ~ 2011	15.5	3,150	-6.9	0
2011 ~ 2012	15.0	2,840	-9.3	0
2012 ~ 2013	18.4	2,640	-8.0	0
2013 ~ 2014	21.7	2,640	-5.8	0
2014 ~ 2015	18.7	2,510	-6.3	0

Table 29 depicts the maximum cooling and heating loads during the harvesting period and the time of occurrence for each year. As the harvesting period of Irwin mango is in the spring, the maximum cooling load and heating load occurred most evenly as compared to those in the other growth periods. The maximum cooling load usually occurred at around 12:00 PM to 2:00 PM and the maximum heating load usually occurred around 4:00 AM to 5:00 AM. The average maximum cooling load was 296,884 kJ/hr and the average maximum heating load was 281,020 kJ/hr.

Table 29 Maximum energy loads of the harvesting period

Year	Maximum cooling loads		Maximum heating loads	
	Loads (kJ/hr)	Occurrence	Loads (kJ/hr)	Occurrence
2006 ~ 2007	279,128	May 28, 2007 13:00	288,202	Apr. 17, 2007 05:00
2007 ~ 2008	267,767	May 02, 2008 13:00	256,208	Apr. 27, 2008 04:00
2008 ~ 2009	311,947	May 28, 2009 13:00	279,943	Apr. 17, 2009 04:00
2009 ~ 2010	299,993	May 21, 2010 13:00	317,290	Apr. 17, 2010 05:00
2010 ~ 2011	311,415	May 29, 2011 12:00	272,818	Apr. 17, 2011 04:00
2011 ~ 2012	289,891	Apr. 30, 2012 13:00	270,747	Apr. 17, 2012 04:00
2012 ~ 2013	296,771	May 16, 2013 14:00	323,791	Apr. 15, 2013 05:00
2013 ~ 2014	307,990	May 30, 2014 13:00	239,379	Apr. 15, 2014 05:00
2014 ~ 2015	307,056	May 27, 2015 13:00	280,801	Apr. 17, 2015 04:00
Average	296,884	-	281,020	-

Table 30 is the external air temperature and solar radiation level on the corresponding time when the maximum cooling and heating loads occurred on the harvesting period. In 2008 ~ 2009, when the external air temperature and solar radiation level were relatively high, the maximum cooling load was 311,947 kJ/hr, which is 5.1% higher than the average maximum cooling load. Moreover, in 2014 ~ 2015, when the external solar radiation was highest and in 2010 ~ 2011, when the external air temperature was highest, the maximum cooling loads were higher than the average maximum cooling load. However in the periods of 2007 ~ 2008, when the external air temperature was lowest, the maximum cooling load was 267,767 kJ/hr, which is 9.8% lower than the average maximum cooling load. In the case of the maximum heating load, in 2012 ~ 2013, when the external air temperature was lowest, the maximum heating load was 323,791 kJ/hr, i.e., 15.2% higher than the average maximum heating load. In contrast during the period of 2013

～ 2014, when the external air temperature was highest, the maximum heating load was 239,379 kJ/hr, which is 14.8% lower than the average maximum heating load.

Table 30 Weather condition of the harvesting period when maximum energy loads occurred

Year	Maximum cooling loads		Maximum heating loads	
	Air temperature (℃)	Solar radiation (kJ/hr)	Air temperature (℃)	Solar radiation (kJ/hr)
2006 ～ 2007	25.8	2,800	2.6	0
2007 ～ 2008	24.5	3,050	4.0	0
2008 ～ 2009	27.8	3,090	1.9	0
2009 ～ 2010	27.0	3,200	0.2	0
2010 ～ 2011	27.3	3,320	2.5	0
2011 ～ 2012	26.6	3,200	1.8	0
2012 ～ 2013	27.3	2,730	-0.8	0
2013 ～ 2014	28.5	2,900	5.8	0
2014 ～ 2015	28.6	2,890	2.1	0

According to the analysis of the maximum energy loads, there was a considerable difference between each maximum energy load depending on the external air temperature and solar radiation (Table 19 ～ Table 30). The periodic energy loads were affected by the average weather conditions during the analysis period, while the maximum energy loads were affected by the limiting value of a specific period. Thus, the tendency of the energy loads by year was different for the periodic energy loads and the maximum energy loads. The maximum cooling load occurred mainly at around 12:00 PM to 2:00 PM, when the external air temperature and solar radiation level were high, while the maximum heating load occurred mainly from 4:00 AM to 7:00 AM, before the sunrise. Among the great number of hourly energy loads calculated by the validated greenhouse BES model and from weather data spanning ten years, last five-year data were used to suggest proper scale of the heat pump in the greenhouse. The maximum cooling load was 518,703 kJ/hr, occurring on August 19, 2010, at 1:00 AM, and the maximum heating load was

469,872 kJ/hr, occurring on February 19, 2012, at 6:00 AM. According to the NIAE of the RDA of Korea, the capacity of a heat pump in a greenhouse should set within 70% of the maximum energy load of last five years. Therefore, the proper performance of the heat pump in the target greenhouse is as follows: approximately 363,092 kJ/hr for the cooling capacity and 328,910 kJ/hr for the heating capacity. However, the performance of the heat pump in the target greenhouse showed a – maximum cooling capacity of 467,381 kJ/hr (3.6 kJ/hr/W × 43,276 W × three units) and a maximum heating capacity of 397,267 kJ/hr (3.6 kJ/hr/W × 36,786 W × three units). The design of the heat pump in the target greenhouse was excessively by about 104,289 kJ/hr (28.7% of the proper performance) in terms of the cooling capacity and by approximately 68,357 kJ/hr (20.8% of the proper performance) in terms of the heating capacity. This reason stems from the method used to calculate the energy load of the greenhouse. The calculation method provided by the NIAE is based on a static design method and does not consider the energy exchange by plants in the greenhouse. Lee (2012) determined that the maximum heating loads as calculated by a static design method were overestimated by 37 ~ 55% compared to the maximum heating loads calculated by a dynamic design method. In addition, Lee (2012) did not consider the plants or the thermal screen in the greenhouse; therefore, the difference between the proper performance of the heat pump as calculated by the greenhouse BES model in this study and the performance of the heat pump in the target greenhouse is explainable. However, the difference in the heat pump performance levels likely cause some economic loss; hence, it is important to calculate energy loads of greenhouses using a dynamic design method for a more feasible heat pump design.

4.5. Differences in greenhouse energy loads depending on whether the energy exchange by plants is considered

Plants in greenhouses mainly absorb thermal energy in the daytime and release thermal energy at night. Many researchers who study energy balances in greenhouses emphasize that a large portion of radiation which penetrates the cladding is use for transpiration by crops (Garzoli and Blackwell, 1973; Boulard and Baille, 1987; Kittas et al., 2003, 2005; Al-Helal and Abdel-Ghany, 2011). The energy loads of a greenhouse can be defined as the required energy used to maintain the internal air temperature against the heat transfer by conduction, radiation, and convection. If crops in the greenhouse are assumed that not to exchange energy with ambient air, this energy will change the energy loads of the greenhouse. Therefore, to calculate the energy loads of greenhouses more accurately, the energy flow from the plants should be considered precisely. However, as noted in the literature review, most researches which simulate energy balances in greenhouses and calculate the energy loads of greenhouses do not consider the energy exchange by crops or do not consider the characteristics of cultivated crops, instead calculating the energy exchange by crops based on the findings of earlier research. In the present study, the characteristics of Irwin mango plants, such as the LAI, stomatal resistance, and the shape of the leaves, are considered in the design of the plant energy exchange model. Therefore, the periodic and maximum energy loads were compared considering the existence of crops to determine the effect of the plants on the energy loads of the greenhouse. The annual and the maximum energy loads of the target greenhouse considering the existence of crops are shown in Fig. 38 ~ Fig. 41.

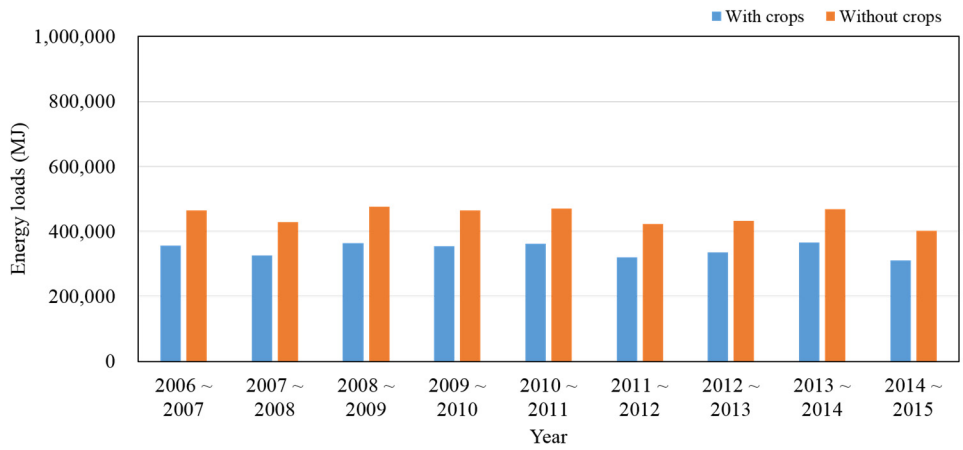

Fig. 38 Annual cooling loads of the target greenhouse considering the existence of crops

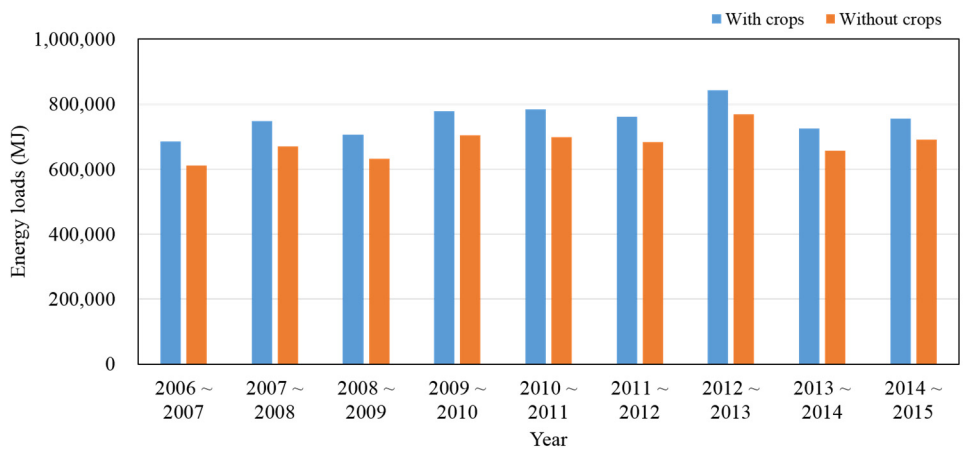

Fig. 39 Annual heating loads of the target greenhouse considering the existence of crops

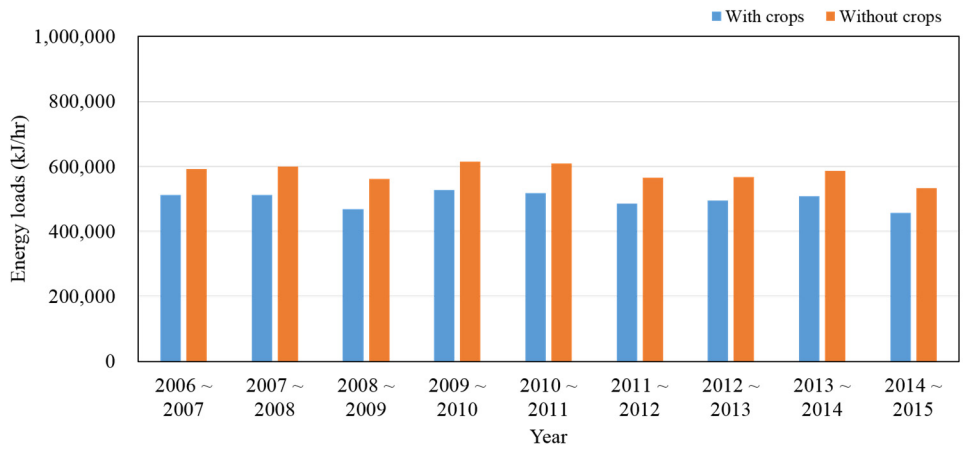

Fig. 40 Maximum cooling loads of the target greenhouse considering the existence of crops

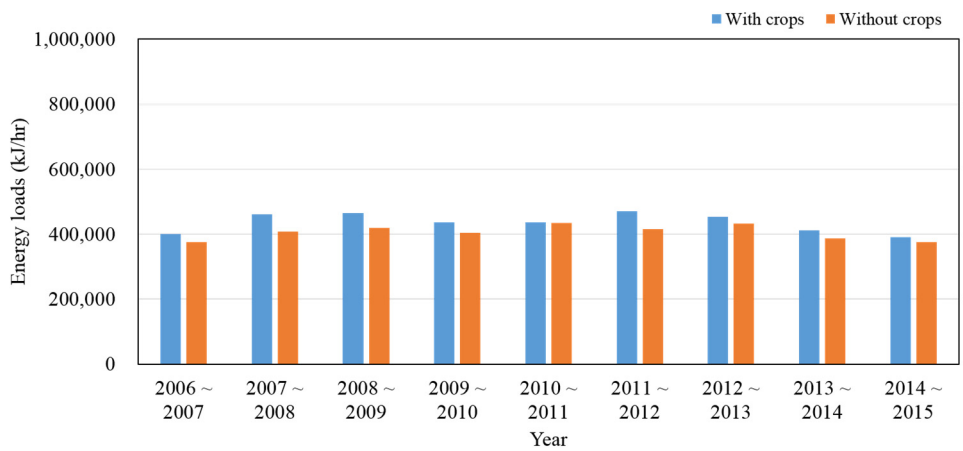

Fig. 41 Maximum heating loads of the target greenhouse considering the existence of crops

Table 31 The rates of change in the periodic and maximum energy loads given the existence of crops

Year	The rate of change for cooling loads (%)		The rate of change for heating loads (%)	
	Annual	Maximum	Annual	Maximum
2006 ~ 2007	23.33	13.60	-11.98	-6.59
2007 ~ 2008	24.02	14.63	-11.63	-13.47
2008 ~ 2009	23.41	16.42	-11.66	-10.93
2009 ~ 2010	23.90	14.18	-10.68	-8.06
2010 ~ 2011	23.04	14.78	-12.41	-0.51
2011 ~ 2012	24.35	14.23	-11.56	-13.12
2012 ~ 2013	22.32	12.72	-9.82	-4.73
2013 ~ 2014	21.93	13.53	-10.29	-6.81
2014 ~ 2015	22.83	14.12	-9.41	-3.90
Average	23.23	14.25	-11.02	-7.56

Table 31 shows the rate of change for the energy loads when not considering the crops in the greenhouse compared to those when accounting for the energy exchange by crops. The annual and the maximum corresponding cooling loads were increased by 23.23 and 14.25% on average when assuming that the crops are not in cultivation. The cultivated crops of the greenhouse BES model used in this study were modeled to absorb thermal energy at the proportion of external radiation at daytime and with a constant value at night. As the cooling load usually occurred during the daytime, the energy absorbed by crops reduces the cooling loads. For the same reason, the energy absorbed by crops at night increases the heating loads; therefore, the corresponding annual and the maximum heating loads were decreased by 11.02 and 7.56% on average when assuming that the crops are not in cultivation.

4.6. Comparative analysis of energy costs according to the energy source

The energy costs were compared according to the type of energy source, in this case kerosene and thermal effluent – heat pump system based on the calculated annual energy loads. The analysis period was the period of 2010 ~ 2014, when the temperature data of the thermal effluent were logged. The periodic energy loads as calculated above were analyzed from the 1st of June to the 31st of May based on the growth stage of Irwin mango plants; however, the energy costs were analyzed from the 1st of January to the 31st of December based on the thermal effluent data. The boiler was set to use kerosene, which is most common in the greenhouses of South Korea. The caloric value of the kerosene boiler was set to 9,200 kcal/L and the average daily oil price was used to calculate the energy cost. The price of electricity to operate the heat pump was set to 41.9 won/kWh based on the agricultural electricity price. The annual energy usage and cost are shown in Table 32.

Table 32 Comparative analysis of energy costs according to the energy source

Year	Boiler		Heat pump		Energy saving cost (won/year)
	Fuel usage (L/year)	Energy cost (won/year)	Electricity usage (kWh/year)	Energy cost (won/year)	
2010	20,225	21,534	211,814	8,875	12,659 (58.79%)
2011	19,883	25,507	150,627	6,311	19,196 (75.26%)
2012	21,391	29,793	211,755	8,873	20,921 (70.22%)
2013	21,147	29,075	210,668	8,827	20,248 (69.64%)
2014	18,940	24,610	205,459	8,609	16,001 (65.02%)
Average	20,317	26,104	198,065	8,299	17,805 (68.21%)

The average energy cost when using the thermal effluent – heat pump system was found to be 68.21% lower compared when a kerosene boiler was used. Table 33 shows the annual average oil price, the sea water temperature, and the thermal effluent temperature. The effect of the temperature of the sea water on the thermal

effluent was minor; however, the oil price has a considerable influence on the energy savings. In 2010, when the oil price was relatively low, the energy consumption reduction ratio when using the thermal effluent – heat pump system was 58.79%, i.e., more than 50%. The instability of greenhouses in South Korea, which are fundamentally vulnerable to changes in world oil prices, can be determined with the application of the thermal effluent – heat pump system based on these results.

Table 33 Annual average of input data for the energy cost analysis

Year	Tax free oil price (won/L)	Temperature of sea water (℃)	Temperature of thermal effluent (℃)
2010	1,071	14.7	24.3
2011	1,327	14.4	24.2
2012	1,394	14.7	24.2
2013	1,365	14.5	24.4
2014	1,300	14.9	21.7
Average	1,291	14.6	23.8

5. Conclusion

In this study, dynamic energy loads of a greenhouse were calculated as an essential prerequisite to apply renewable energy sources such as thermal effluent to greenhouses. A greenhouse dynamic BES model was designed and validated to calculate the periodic energy loads the maximum energy loads. The target greenhouse was an eight-span plastic-covered greenhouse which used thermal effluent from a thermal power plant on a trial basis. The greenhouse BES model was validated based on field experiments. The periodic and the maximum energy loads were calculated based on the validated greenhouse BES model and on ten years of weather data. The annual energy loads were used to analyze the energy cost when using the thermal effluent – heat pump system compared to a kerosene boiler system. The maximum energy loads were used to suggest the proper performance of a heat pump in the greenhouse and determine the influence of the energy exchange by plants on the energy loads of the greenhouse.

The greenhouse dynamic BES model was designed the commercial BES program TRNSYS. The model was designed in three parts; greenhouse structural modeling, crop energy exchange modeling, and thermal effluent – heat pump modeling. To design the greenhouse BES mode, field experiments were conducted to measure the structural characteristics of the greenhouse, in this case the shape, cladding, HVAC system as well as the crop characteristics of the stomatal resistance, LAI and the working schedule of the thermal screen, heat pump and ventilator in the greenhouse. The micro-climate of the target greenhouse and the transpiration rate of the cultivated crops were measured to validate the model. The designed crop energy exchange model was verified based on at comparison of the transpiration rate, which provides a good estimate of the change of the transpiration rate, throughout the experimental period (R^2 = 0.96, d = 0.99). The methodology of the design and validation of the plant energy exchange model was verified. Accordingly, it will be useful to consider cultivated crops in greenhouses when designing a dynamic energy

exchange model for greenhouses. The overall greenhouse dynamic BES model was also verified by comparing the greenhouse internal air temperature as measured in a field experiment. The designed model was found to be able to provide a good estimate of changes of the internal air temperature of the greenhouse (R^2 = 0.97, d = 0.99).

The validated greenhouse dynamic BES model and weather data spanning ten years were used to calculate the periodic and the maximum energy loads of the target greenhouse. The periodic energy loads of six growth periods (vegetation, floral-initiation, flowering, fruit-bearing, fruit-growing, harvesting) differed with the weather conditions of each year. The optimum growth temperature of Irwin mango, as cultivated in the target greenhouse, was usually in the range of 20 to 30 ℃; therefore, the cooling loads mainly occurred in the summer season and the heating loads mainly occurred in the winter season. However, though the floral-initiation period of Irwin mango in the target greenhouse starts in the autumn, the optimum growth temperature range is decreased to 8 ~ 20 ℃; therefore, heating loads seldom occurred, and the periodic cooling loads were highest as compared to the other growth periods, representing 54.1% of the annual cooling load. The calculated annual energy loads were used to analyze the energy cost with two energy sources, a kerosene boiler of the type most commonly used in the greenhouses of South Korea, and the thermal effluent – heat pump system which is applied in the target greenhouse. The average energy cost when using the thermal effluent – heat pump system was analyzed and found to be 68.21% lower compared to the use of the kerosene boiler. For this reason, the vulnerability of greenhouses in South Korea to changes in world oil prices could be relieved by using the thermal effluent – heat pump system.

The maximum cooling load occurred mainly at around 12:00 PM to 2:00 PM, and the maximum heating load occurred mainly from 4:00 AM to 7:00 AM. Among the hourly energy loads for a five-year period, the maximum cooling and maximum heating loads were 518,703 and 469,872 kJ/hr, respectively. The proper performance

of the heat pump was found to be 363,092 kJ/hr in terms of the cooling capacity and 328,910 kJ/hr in terms of the heating capacity according to the standard, which suggests the proper scale of a heat pump in a greenhouse according to the NIAE of the RDA. The performance of the heat pump in the target greenhouse was 467,381 kJ/hr for the maximum cooling capacity and 397,267 kJ/hr for the maximum heating capacity; a design which was excessive by approximately 28.7 and 20.8%, respectively, with regard to the proper performance as calculated in this study. These results came from the method used to calculate the energy load of the greenhouse. The calculation method which was provided by the NIAE is based on a static design method, which may overestimate the maximum energy compared to that calculated by a dynamic design method. For this reason, when designing the proper scale of a heat pump in a greenhouse using the static design method, the heating and cooling system can be excessive, leading to economic losses for the farm using it.

The differences in the greenhouse energy loads of the target greenhouse depending on the existence of crops were analyzed. The maximum cooling loads were overestimated by 14.25% and the maximum heating loads were underestimated by 7.56% when assuming that crops in the greenhouse did not exchange energy with the ambient air. As the proper scale of a heat pump in a greenhouse is designed based on the maximum energy load, to design a more feasible heating and cooling system in a greenhouse and to maintain the optimum growth environment for cultivation, the energy exchange between crops and the ambient air should be considered. This will become more important when designing a heating and cooling system for a greenhouse which cultivates more common crops, such as tomatoes and bell peppers, considering that the crops in this study are cultivated in pots and that the plant density is relatively low.

In this study, a dynamic energy exchange between each component in the greenhouse was simulated. These results will be useful when utilizing renewable energy sources, such as geothermal heat, thermal effluent, solar energy and others in to greenhouses. In particular, considering that the proposed plant energy exchange

model which considers specific crops demonstrated the capability of high accuracy, the results here can provide a methodology with which to a design greenhouse dynamic energy exchange model which takes into account all of the major components in the greenhouse.

Bibliography

Ahmadi, G., & Glockner, P. G. (1982). Dynamic simulation of the performance of an inflatable greenhouse in the southern part of Alberta. I. Analysis and average winter conditions. *Agricultural Meteorology,* 27(3-4), 155-180.

Al-Helal, I. M., & Abdel-Ghany, A. M. (2011). Energy partition and conversion of solar and thermal radiation into sensible and latent heat in a greenhouse under arid conditions. *Energy and Building,* 43, 1740-1747.

Arinze, E. A., Schoenau, G. J., & Besant, R. W. (1984). A dynamic thermal performance simulation model of an energy conserving greenhouse with thermal storage. *Transactions of the ASAE,* 27(2), 508-519.

Attar, I., & Farhat, A. (2015). Efficiency evaluation of a solar water heating system applied to the greenhouse climate. *Solar Energy,* 119, 212-224.

Avissar, R., Avissar, P., Mahrer, Y., & Bravdo, B. A. (1985). A model to simulate response of plant stomata to environmental conditions. *Agricultural and Forest Meteorology,* 34(1), 21-29.

Baille, A., López, J. C., Bonachela, S., González-Real, M. M., & Montero, J. I. (2006). Night energy balance in a heated low-cost plastic greenhouse. *Agricultural and forest meteorology,* 137(1), 107-118.

Bot, G. P. (1983). Greenhouse climate: from physical processes to a dynamic model. Ph.D. diss., *Wageningen University,* Wageningen, Netherland.

Boulard, T., & Baille, A. (1987). Analysis of thermal performance of a greenhouse as a solar collector. *Energy in agriculture,* 6(1), 17-26.

Boulard, T., Baille, A., Mermier, M., & Villette, F. (1991). Measurement of stomatal resistance and transpiration in a greenhouse tomato coanopy. Comparison between a 1-layer and multi-layer model. *Agronomie,* 11(4), 259-274.

Candy, S., Moore, G., & Freere, P. (2012). Design and modeling of a greenhouse for a remote region in Nepal. *Procedia Engineering,* 49, 152-160.

Cane, R. L. D. (1979). A "Modified" bin method for estimating annual heating energy requirements of residential air source heat pumps. *ASHRAE Journal,* 21(9), 60-63.

Chen, J., Xu, F., Tan, D., Shen, Z., Zhang, L., & Ai, Q. (2015). A control method for agricultural greenhouses heating based on computational fluid dynamics and energy prediction model. *Applied Energy,* 141, 106-118.

Cho, J. H., Kim, D. Y., & Lee, J. S. (2010). *Directions for developing green aquaculture using thermal effluent from power plant,* Retrieved from http://www.kmi.re.kr

Cho, S. H., Kim, S. S., & Choi, C. Y. (2010). Study on the revision of HDD for 15 main cities of Korea. *Journal of Air-Conditioning and Refrigeration,* 22(7), 436-441.

Christenson, M., Manz, H., & Gyalistras, D. (2006). Climate warming impact on degree-days and building energy demand in Switzerland. *Energy Conversion and Management,* 47, 671-686.

Cooper, P. I. (1969a). Digital simulation of transient solar still processes. *Solar Energy,* 12(3), 313-331.

Cooper, P. I. (1969b). The absorption of radiation in solar stills. *Solar energy,* 12(3), 333-346.

Cooper, P. I., & Fuller, R. J. (1983). A transient model of the interaction between crop, environment and greenhouse structure for predicting crop yield and energy consumption. *Journal of Agricultural Engineering Research,* 28(5), 401-417.

Demrati, H., Boulard, T., Fatnassi, H., Bekkaoui, A., Majdoubi, H., Elattir, H., & Bouirden, L. (2007). Microclimate and transpiration of a greenhouse banana crop. *Biosystems Engineering,* 98(1), 66-78.

Du, J., Bansal, P., & Huang, B. (2012). Simulation model of a greenhouse with a heat-pipe heating system. *Applied energy,* 93, 268-276.

Duncan, G. A., Loewer, O. J., & Colliver, D. G. (1981). Simulation of energy flows in a greenhouse: magnitudes and conservation potential. *Transactions of the ASAE,* 24(4), 1014-1021.

Durmayaz, A., Kadıoğlu, M., & Şen, Z. (2000). An application of the degree-hours method to estimate the residential heating energy requirement and fuel consumption in Istanbul. *Energy,* 25, 1245-1256.

Enerdata. (2016). *Global energy statistical yearbook.* Retrieved from http://yearbook.energydata.net

Fatnassi, H., Boulard, T., & Bouirden, L. (2013). Development, validation and use of a dynamic model for simulate the climate conditions in a large scale greenhouse equipped with insect-proof nets. *Computers and electronics in agriculture,* 98, 54-61.

Fitz-Rodriguez, E., Kubota, C., Giacomelli, G. A., Tignor, M. E., Wilson, S. B., & McMahon, M. (2010). Dynamic modeling and simulation of greenhouse environments under several scenarios: A web-based application. *Computers and electronics in agriculture,* 70(1), 105-116.

Fynn, R. P., Al-Shooshan, A., Short, T. H., & McMahon, R. W. (1993). Evapotranspiration measurement and modeling for a potted chrysanthemum crop. *Transactions of the ASAE,* 36(6), 1907-1913.

Garzoli, K., & Blackwell, J. (1973). Response of a glasshouse to high solar radiation and ambient temperature. *Journal of agricultural engineering research,* 18, 205-216.

Garzoli, K. V., & Blackwell, J. (1981). An analysis of the nocturnal heat loss from a single skin plastic greenhouse. *Journal of Agricultural Engineering Research,* 26(3), 203-214.

Ha, T., Lee, I. B., Kwon, K. S., & Hong, S. W. (2015). Computation and field experiment validation of greenhouse energy load using building energy simulation model. International *Journal of Agricultural and Biological Engineering,* 8(6), 116-127.

Hong, H. K., & Cho, S. H. (2001). Dynamic thermal energy analysis of building. *Journal of Air-Conditioning and Refrigeration,* 13(1), 44-54.

Hong, T., Chou, S. K., & Bong, T. Y. (2000). Building simulation: an overview of developments and information sources. *Building and Environment,* 35, 347-361.

Hunn, B. D. (1996). *Fundamentals of building energy dynamics* (Vol. 4). MIT Press.

Hyun, S. K., Hong, H., & Yoo, H. (2002). Validation experiment and calculation of heating load for a test space. *Korean Journal of Air Conditioning and Refrigeration Engineering,* 14(2), 153-160.

Jarvis, P. G. (1976). The interpretation of the variations in leaf water potential and stomatal conductance found in canopies in the field. *Philosophical Transactions of the Royal Society of London B: Biological Sciences,* 273(927), 593-610.

Jensen, S. Ø. (1995). Validation of building energy simulation programs: a methodology. *Energy and Buildings,* 22(2), 133-144.

Joudi, K. A., & Farhan, A. A. (2015). A dynamic model and an experimental study for the internal air and soil temperatures in an innovative greenhouse. *Energy Conversion and Management,* 91, 76-82.

Jung, D. H., Cho, Y. Y., & Son, J. E. (2016). Estimation of leaf area, fresh and dry weights of Irwin mango grown in greenhouse using leaf length and width, SPAD value, and petiole length. *Proceedings of the Korean Society for Bio-Environment Control Conference,* 25(1), 187-188.

Karlsson, F., Rohdin, P., & Persson, M. L. (2007). Measured and predicted energy demand of a low energy building: important aspects when using building energy simulation. *Building services engineering research and technology,* 28(3), 223-235.

Kavanaugh, S. P. (1998). A design method for hybrid ground-source heat pumps. *American Society of Heating, Refrigerating and Air-Conditioning Engineers transactions,* 104, 691-698.

Kim, B. H., Jo, S. B., & Kim, J. P. (1990). A software development of energy consumption for HVAC system of building. *Magazine of the Society of Air-Conditioning and Refrigerating Engineers of Korea,* 19(2), 67-81.

Kimball, B. A. (1973). Simulation of the energy balance of a greenhouse. *Agricultural Meteorology,* 11, 243-260.

Kindelan, M. (1980). Dynamic modeling of greenhouse environment. *Transactions of the ASAE,* 23(5), 1232-1239.

Kittas, C., Katsoulas, N., & Baille, A. (2003). Influence of an aluminized thermal screen on greenhouse microclimate and canopy energy balance. *Transactions of the ASAE,* 46(6), 1653.

Kittas, C., Karamanis, M., & Katsoulas, N. (2005). Air temperature regime in a forced ventilated greenhouse with rose crop. *Energy and buildings,* 37(8), 807-812.

Korea Energy Economics Institute. (2016). *Yearbook of regional energy statistics*. Retrieved from http://www.keei.re.kr

Krese, G., Prek, M., & Butala, V. (2012). Analysis of building electric energy consumption data using an improved cooling degree day method. *Journal of Mechanical Engineering,* 58(2), 107-114.

Lee, C. S., & Choi, Y. D. (1997). Analysis of energy consumption of office building by thermal resistance-capacitance method. *Journal of Air-Conditioning and Refrigeration,* 9(1), 1-13.

Lee, H. W., Diop, S., & Kim, Y. S. (2011). Variation of the overall heat transfer coefficient of plastic greenhouse covering material. *The Korean Society for Bio-Environment Control,* 20(2), 72-77.

Lee, S. B. (2012). Analysis and validation of dynamic thermal energy for greenhouse with geothermal system using field data. Master diss., *Seoul National University,* Seoul, South Korea.

Luo, W., De Zwart, H. F., Dail, J., Wang, X., Stanghellini, C., & Bu, C. (2005). Simulation of greenhouse management in the subtropics, Part I: Model validation and scenario study for the winter season. *Biosystems Engineering,* 90(3), 307-318.

Mashonjowa, E., Ronsse, F., Milford, J. R., & Pieters, J. G. (2013). Modelling the thermal performance of a naturally ventilated greenhouse in Zimbabwe using a dynamic greenhouse climate model. *Solar Energy,* 91, 381-393.

Mesmoudi, K., Soudani, A., Zitouni, B., Bournet, P. E., & Serir, L. (2010). Experimental study of the energy balance of unheated greenhouse under hot and arid climates: Study for the night period of winter season. *Journal of the Association of Arab Universities for Basic and Applied Sciences,* 9(1), 27-37.

Meyer, B. S., & Anderson, D. B. (1952). Plant Physiology, 2nd edn Van Nostrand. *New York.*

Mihara, Y., (1978). Computation formulae for greenhouse heating degree-hour with consideration for sunshine. *Journal of Agricultural Meteorology,* 34(2), 83-85.

Ministry of Agriculture, Food and Rural Affairs. (2015a). *Greenhouse cultivation present condition and product statistic.* Retrieved from http://www.mafra.go.kr

Ministry of Agriculture, Food and Rural Affairs. (2015b). *Project for improve use efficiency of agricultural energy,* Retrieved from http://www.mafra.go.kr

Monteith, J. L. (1964, December). Evaporation and environment. In *Symposia of the society for experimental biology* (Vol. 19, pp. 205-234).

Moon, S. H., & Park, B. J. (1984). On the heating degree days. *Architectural Institute of Korea,* 30, 83-86.

Nam, S. W., & Shin, H. H. (2015). Development of a method to estimate the seasonal heating load for plastic greenhouses. *Journal of the Korean Society of Agricultural Engineers,* 57(5), 37-42.

Ntinas, G. K., Fragos, V. P., & Nikita-Martzopoulou, Ch. (2014). Thermal analysis of a hybrid solar energy saving system inside a greenhouse. *Energy Conversion and Management,* 81, 428-439.

Ortiz-Ospina, E., & Roser, M. (2016). *World population growth.* Retrieved from http://ourworldindata.org/world-population-growth

Papadakis, G., Frangoudakis, A., & Kyritsis, S. (1989). Theoretical and experimental investigation of thermal radiation transfer in polyethylene covered greenhouses. *Journal of Agricultural Engineering Research,* 44, 97-111.

Parent, M. (2001). A simplified tool for assessing the feasibility of ground-source heat pump projects. *ASHRAE Transactions,* 107, 120-129.

Park, S. J. (2015). Development and analysis of BES dynamic design method of a cogeneration plant using livestock manure. Master diss., *Seoul National University,* Seoul, South Korea.

Penman, H. L. (1948, April). Natural evaporation from open water, bare soil and grass. In *Proceedings of the Royal Society of London A: Mathematical, Physical and Engineering Sciences* (Vol. 193, No. 1032, pp. 120-145). The Royal Society.

Prenger, J. J., Fynn, R. P., & Hansen, R. C. (2002). A comparison of four evapotranspiration models in a greenhouse environment. *Transactions of the ASAE,* 45(6), 1779.

Reddy, T. A., Maor, I., & Panjapornpon, C. (2007). Calibrating detailed building energy simulation programs with measured data—Part I: General methodology (RP-1051). *Hvac&R Research,* 13(2), 221-241.

Rijtema, P. E. (1965). *An analysis of actual evapotranspiration.* Center for Agricultural Publications and Documentation.

Sarak, H., & Satman, A. (2003). The degree-day method to estimate the residential heating natural gas consumption in Turkey: a case study. *Energy,* 28, 929-939.

Seginer, I., & Levav, N. (1971). Models as tools in greenhouse climate design. Technion-Israel Institute of Technology, Haifa, Israel. *Agricultural Engineering Station, Publication,* (115).

Sethi, V. P. (2009). On the selection of shape and orientation of a greenhouse: Thermal modeling and experimental validation. *Solar Energy,* 83, 21-38.

Singh, G., Singh, P. P., Lubana, P. P. S., & Singh, K. G. (2006). Formulation and validation of a mathematical model of the microclimate of a greenhouse. *Renewable Energy,* 31(10), 1541-1560.

Song, S. Y., Koo, B. K., & Lee, B. I. (2009). Analysis of annual heating load reduction effect for thermal bridge-free externally insulated apartment buildings using the steady-state method. *Architectural Institute of Korea,* 25(8), 365-372.

Stanghellini, C. (1987). Transpiration of greenhouse crops; an aid to climate management. Ph.D. diss., *Wageningen University,* Wageningen, Netherland.

Thamilseran, S., & Haberl, J. S. (1994). A bin method for calculating energy conservation retrofit savings in commercial buildings. *Proceedings of the 9th Symposium on Improving Building Systems in Hot and Humid Climates*. Retrieved from http://oaktrust.library.tamu.edu

Van der Veken, J., Saelens, D., Verbeeck, G., & Hens, H. (2004). Comparison of steady-state and dynamic building energy simulation programs. In *Proceedings of the international Buildings IX ASHRAE conference on the performance of exterior envelopes of whole buildings, Clearwater Beach, Florida 2004.*

Walker, J. N. (1965). Predicting temperatures in ventilated greenhouses. *Transactions of the ASAE, 8(3),* 445-0448.

Wang, Z., Ding, Y., Geng, G., & Zhu, N. (2014). Analysis of energy efficiency retrofit schemes for heating, ventilating and air-conditioning systems in existing office buildings based on the modified bin method. *Energy Conversion and Management,* 77, 233-242.

Whittle, R. M., & Lawrence, W. J. C. (1960). The climatology of glasshouses, III. Air temperature. *Journal of Agricultural Engineering Research,* 5, 165-178.

Woo, Y. H., Kim, D. E., Lee, S. Y., Kim, T. Y., & Chang, H. K. (1998). The study on greenhouse heating load modelling according to region in Korea. *Bulletin of horticultural experiment research* (pp. 1021-1041). National Horticultural Research Institute, Rural Development Administration, South Korea.

국문 초록

작물 에너지교환을 고려한 온실 에너지모델 설계 및 에너지부하 산정

이 승 노
생태조경·지역시스템공학부 지역시스템공학 전공
서울대학교 대학원

우리나라의 온실재배면적은 지난 몇 십년 동안 급격하게 증가하였으며 대부분의 온실에서 화석연료를 에너지원으로 작물의 적정생육환경을 조성하고 있다. 화석연료를 대체할 새로운 에너지원에 대한 관심이 세계적으로 증가함에 따라 최근 국내 온실 산업에서도 신재생에너지를 온실의 냉난방장치에 접목하려는 시도가 수행되어 왔다. 신재생에너지의 시기별 가용 에너지량을 효율적으로 활용하기 위해서는 온실 내 재배작물 및 생육단계에 따른 시기별 에너지부하 산정이 필요하다. 그러나 온실 내 유입되는 에너지 중 상당 부분이 작물의 증산에 사용됨에도 불구하고 기존의 온실 에너지부하 산정 과정에서는 작물을 전혀 고려하지 않거나 각 온실 내 재배되는 작물 별 특성을 반영하지 않고 단순히 선행연구의 결과를 이용하는 데에 그치고 있다.

본 연구에서는 온실에 새로운 에너지원을 적용하기 위한 선행연구로써 온실의 동적 에너지교환 모델을 설계하였으며 이를 이용하여 시간별 에너지부하를 산정하였다. 이를 위한 타당한 연구 방법을 정립하기 위해서 건물의 에너지부하 산정법, 온실 내 에너지평형, 작물 에너지교환 모델에 관련된 연구사 분석을 수행하였다.

본 연구의 대상 온실은 보령화력발전소 인근에 위치한 8 연동

플라스틱 온실로 발전소로부터 방류되는 온배수의 열에너지를 이용하여 시범적으로 냉난방장치를 가동하고 있다. 온실의 동적 에너지교환 모델 설계 및 검증을 위해서 수차례의 현장실험을 수행하였다. 현장실험을 통해서 온실의 구조적 특징, 내부 설비의 가동 조건, 재배 작물의 특성 등을 측정하였다. 온실 에너지교환 모델은 상용 건물에너지시뮬레이션 (Building Energy Simulation; BES) 프로그램인 TRNSYS를 이용하여 설계하였으며 온실 구조, 작물 에너지교환, 온배수 – 히트펌프 시스템으로 구분지어 설계하였다. 대상 온실 내 재배되는 애플 망고 (Irwin mango)에 의한 에너지교환을 구현하기 위해서 현장실험을 통해서 평균 엽면적지수를 측정하였으며 기공저항의 회귀식을 도출하였다. 설계한 모델의 검증을 위해서 온실 내외부 기온 및 일사량 등 미기상을 측정하였다. 작물 에너지교환 모델은 증산량을 이용하여 검증하였으며 온실 동적 에너지교환 모델은 온실 내부 기온을 이용하여 검증을 수행하였다. 검증 결과 작물 에너지교환 모델은 실제 작물의 증산량을 잘 모의하는 것으로 확인하였으며 (R^2 = 0.96, d = 0.99) 온실 동적 에너지교환 모델은 온실 내부 기온의 변화를 잘 모의하는 것으로 확인하였다 (R^2 = 0.97, d = 0.99).

검증된 온실 에너지교환 모델과 10년치의 기상자료를 이용하여 시간별 에너지부하를 산정하였다. 작물의 생육단계별 에너지부하를 합산하여 기간 에너지부하를 산정하였으며 각 생육단계별 최대에너지부하를 분석하였다. 기간별 에너지부하는 에너지원에 따른 에너지비용의 비교분석에 활용되었으며 분석 결과 온배수 – 히트펌프 시스템을 활용할 경우 국내 온실에서 가장 보편적으로 사용되는 등유보일러와 비교하여 평균 68.21%의 에너지비용 절감 효과를 확인하였다. 농촌진흥청 산하 농업공학연구소에 따르면 온실 내 히트펌프의 적정설계용량은 과거 5년치의 기상자료를 통해 산정된 최대 냉난방부하의 70%로 설정된다. 지난 5년간의 최대 냉난방부하는 각각 518,703, 469,872 kJ/hr로 분석되었으며 히트펌프의 적정 냉난방 설계 용량은 각각 363,042, 328,910 kJ/hr로 파악되었다. 산정된 적정설계용량과 대상 온실 내 설치되어 있는

히트 펌프의 정격 용량을 비교한 결과 냉난방설계용량이 각각 28.7, 20.8% 과다 설계되었음을 확인하였다. 이는 최대에너지부하를 산정하는 방법론에서 기인한 것으로 분석되었다. 또한 온실 내 작물의 에너지교환이 에너지부하에 미치는 영향을 파악하기 위해서 작물 에너지교환 구현 유무에 따른 에너지부하를 비교분석하였다. 분석 결과 작물을 고려하지 않을 경우 기간 및 최대 냉방부하는 평균적으로 23.23, 14.25% 과다 산정되었으며 기간 및 최대 난방부하는 평균적으로 11.02, 7.56% 과소 산정됨을 확인하였다. 이를 통해서 온실의 에너지 사용량을 보다 정확하게 예측하기 위해서는 온실의 에너지교환 모델 설계 및 에너지부하를 산정할 경우 재배 작물의 에너지교환을 반드시 고려해야할 것으로 판단된다.

주요어: 건물에너지시뮬레이션, 신재생에너지, 에너지부하, 온실, 작물 에너지교환 모델,

학 번: 2015-21756